SAND2013-8544C

On the Development of a Scalable Fully-implicit Stabilized Unstructured FE Capability for Resistive MHD with Integrated Adjoint Error-Estimation

John N. Shadid

Computational Science and Applied Mathematics Group,
Sandia National Laboratories

Collaborators:

Roger P. Pawlowski, Eric C. Cyr
Tom M. Smith, Tim M. Wildey
Paul T. Lin, R. S. Tuminaro

Sandia National Laboratories

Luis Chacon

Los Alamos National Laboratory

Don Estep and Jehanzeb Chaudhry

Colorado State University

Outline

- **General Scientific and Mathematical/Computational Motivation**
- **Overview of 3D Resistive MHD Equations and VMS/Stabilized FE formulation**
- **Motivation for Fully Implicit Newton – Krylov Solution Methods**
    - **General comments**
    - **Solving a wide range of flow conditions (Boussinesq, Anelastic, Low-Mach)**
    - **Facilitating adjoint methods for error-estimation and sensitivity analysis**
- **Scaling of Fully-coupled AMG preconditioner**
- **Results for Preliminary Simulations for Geodynamo Relevant Flow Mechanisms**
    - **Rotating thermal convection in spherical geometry**
    - **High Rayleigh number thermal convection (validation w/lab experiments)**
- **Results for Plasmoid Instability of this Current Sheets at High Lunquist numbers**
- **Conclusions**

Sandia National Laboratories

Motivation

Scientific / Technology: Resistive and extended MHD equations are used to model a variety of important plasma physics systems

- **Astrophysics: Solar flares, sunspots, magnetic reconnection**
- **Geophysics: Earth's magnetospheric sub-storms, geo-dynamo**
- **Fusion: Magnetic confinement (ITER - Tokamak), Inertial conf. (NIF, Z-pinch)**
- **Technology/Engineering: Plasma Reactors, MHD Pumps, ..**

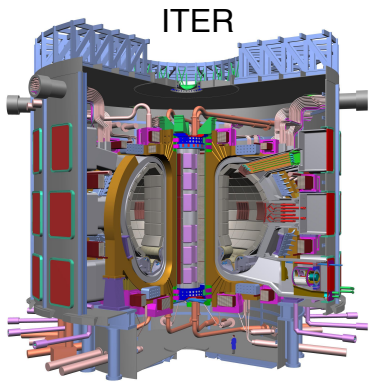

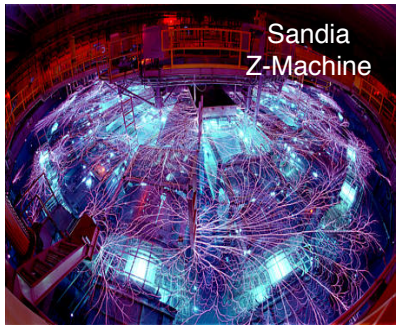

Mathematical / Computational Motivation: Achieving Scalable Predictive Simulations of Complex Highly Nonlinear Multiphysics Systems to Enable Scientific Discovery and Engineering Design/ Optimization

Our goal is to develop:

- **Stable and higher-order accurate fully-implicit formulations,**
- **Robust fully-coupled nonlinear/linear iterative solution methods,**
- **Scalable and efficient parallel preconditioners,**
- **Integrated sensitivity and error-estimation to enable UQ capabilities.**

Sandia National Laboratories

One Fluid Resistive MHD Equations

Resistive MHD Model in Residual Notation

$$\mathbf{R_u} = \frac{\partial \rho \mathbf{u}}{\partial t} + \nabla \cdot [\rho \mathbf{u} \otimes \mathbf{u} - (\mathbf{T} + \mathbf{T}_M)] + 2\rho\Omega \times \mathbf{u} - \rho \mathbf{g} = \mathbf{0}; \quad \mathbf{T} = -\left(P + \frac{2}{3}\mu(\nabla \bullet \mathbf{u})\right)\mathbf{I} + \mu[\nabla \mathbf{u} + \nabla \mathbf{u}^T]$$

$$\mathbf{T_M} = \frac{1}{\mu_0}\mathbf{B} \otimes \mathbf{B} - \frac{1}{2\mu_0}\|\mathbf{B}\|^2 \mathbf{I}$$

$$R_P = \frac{\partial \rho}{\partial t} + \nabla \cdot (\rho \mathbf{u}) = 0$$

$$R_e = \frac{\partial (\rho e)}{\partial t} + \nabla \cdot [\rho \mathbf{v} e + \mathbf{q}] - \mathbf{T} : \nabla \mathbf{v} - \eta \| \frac{1}{\mu_0} \nabla \times \mathbf{B} \|^2 = 0$$

$$\frac{\partial \mathbf{B}}{\partial t} + \nabla \times \mathbf{E} = \mathbf{0}; \; \mathbf{J} = \tfrac{1}{\mu_0} \nabla \times \mathbf{B}; \; \mathbf{E} = -\underbrace{\mathbf{u} \times \mathbf{B}}_{\text{Ideal}} + \underbrace{\eta \mathbf{J}}_{\text{Resistive}} + \underbrace{\frac{d_i}{n}(\mathbf{J} \times \mathbf{B} - \nabla P_e)}_{\text{Hall}} + \underbrace{\frac{d_e^2}{n}\frac{d\mathbf{J}}{dt}}_{\text{e inertia}}$$

Sandia National Laboratories

Resistive MHD Equations

Resistive MHD Model in Residual Notation

$$\mathbf{R_u} = \frac{\partial \rho \mathbf{u}}{\partial t} + \nabla \cdot [\rho \mathbf{u} \otimes \mathbf{u} - (\mathbf{T} + \mathbf{T}_M)] + 2\rho\Omega \times \mathbf{u} - \rho \mathbf{g} = \mathbf{0}; \quad \mathbf{T} = -\left(P + \frac{2}{3}\mu(\nabla \bullet \mathbf{u})\right)\mathbf{I} + \mu[\nabla \mathbf{u} + \nabla \mathbf{u}^T]$$

$$\mathbf{T_M} = \frac{1}{\mu_0}\mathbf{B} \otimes \mathbf{B} - \frac{1}{2\mu_0}\|\mathbf{B}\|^2 \mathbf{I}$$

$$R_P = \frac{\partial \rho}{\partial t} + \nabla \cdot (\rho \mathbf{u}) = 0$$

$$R_e = \frac{\partial (\rho e)}{\partial t} + \nabla \cdot [\rho \mathbf{v} e + \mathbf{q}] - \mathbf{T} : \nabla \mathbf{v} - \eta \| \frac{1}{\mu_0} \nabla \times \mathbf{B} \|^2 = 0$$

$$\mathbf{R_B} = \frac{\partial \mathbf{B}}{\partial t} - \nabla \times (\mathbf{u} \times \mathbf{B}) + \nabla \times (\frac{\eta}{\mu_0} \nabla \times \mathbf{B}) = \mathbf{0}.$$

- Complex coupled multiphysics system
  - Highly nonlinear
  - multiple-time and -length scales
  - Elliptic, parabolic and hyperbolic character in different parameter ranges

Sandia National Laboratories

Resistive MHD Equations

Resistive MHD Model in Residual Notation

$$\mathbf{R_u} = \frac{\partial \rho \mathbf{u}}{\partial t} + \nabla \cdot [\rho \mathbf{u} \otimes \mathbf{u} - (\mathbf{T} + \mathbf{T}_M)] + 2\rho\Omega \times \mathbf{u} - \rho \mathbf{g} = \mathbf{0}; \quad \mathbf{T} = -\left(P + \frac{2}{3}\mu(\nabla \bullet \mathbf{u})\right)\mathbf{I} + \mu[\nabla \mathbf{u} + \nabla \mathbf{u}^T]$$

$$\mathbf{T_M} = \frac{1}{\mu_0}\mathbf{B} \otimes \mathbf{B} - \frac{1}{2\mu_0}\|\mathbf{B}\|^2 \mathbf{I}$$

$$R_P = \frac{\partial \rho}{\partial t} + \nabla \cdot (\rho \mathbf{u}) = 0$$

$$R_e = \frac{\partial (\rho e)}{\partial t} + \nabla \cdot [\rho \mathbf{v} e + \mathbf{q}] - \mathbf{T} : \nabla \mathbf{v} - \eta \| \frac{1}{\mu_0} \nabla \times \mathbf{B} \|^2 = 0$$

$$\mathbf{R_B} = \frac{\partial \mathbf{B}}{\partial t} + \nabla \cdot \left[\mathbf{u} \otimes \mathbf{B} - \mathbf{B} \otimes \mathbf{u} - \frac{\eta}{\mu_0}\left(\nabla \mathbf{B} - (\nabla \mathbf{B})^T\right) + \psi \mathbf{I}\right] = \mathbf{0}$$

$$R_\psi = \nabla \cdot \mathbf{B} = 0$$

- Divergence free involution enforced as elliptic constraint with a Lagrange multiplier.
(Dedner et. al. 2002; Codina et. al. 2006, 2011)
    - Only weakly divergence free in FE implementation (stabilization of B - ψ coupling)

- Can show relationship with projection (e.g. Brackbill and Barnes 1980) when 1st order-splitting is used.

- Issue for using C0 FE for domains with re-entrant corners / soln singularities
(Costabel et. al. 2000, 2002, Codina, 2011

Sandia National Laboratories

Summary of Initial Stabilized FE Weak form of Equations for Low Mach Number MHD System;

Governing Equation	Stabilized FE Residual (following Hughes et. al., Shakib - Navier-Stokes; Salah et. al. 99 & 01, Codina et. al. 2006 -Magnetics)
Momentum	$F_{m,i} = \int_{\Omega} \Phi R_{m,i}\, d\Omega + \sum_e \int_{\Omega^e} \rho\tau_m \left(\mathbf{u}\bullet\nabla\Phi\right) R_{m,i}\, d\Omega + \sum_e \int_{\Omega^e} \nu_{m,i} \nabla\Phi \bullet \mathbf{C}^c \nabla u_i\, d\Omega$
Total Mass	$F_P = \int_{\Omega} \Phi R_P\, d\Omega + \sum_e \int_{\Omega^e} \rho\tau_m \nabla\Phi \bullet \mathbf{R_m}\, d\Omega$ $\sum_e \int_{\Omega^e} \rho\tau_m \nabla\Phi \cdot \left[\frac{\partial(\rho\mathbf{v})}{\partial t} + \nabla\cdot[\rho\mathbf{v}\otimes\mathbf{v}] + \nabla P - \nabla\cdot\Pi - \mathbf{J}\times\mathbf{B}\right] d\Omega$
Thermal Energy	$F_T = \int_{\Omega} \Phi R_T\, d\Omega + \sum_e \int_{\Omega^e} \rho C_P \tau_T \left(\mathbf{u}\bullet\nabla\Phi\right) R_T\, d\Omega + \sum_e \int_{\Omega^e} \nu_T \nabla\Phi \bullet \mathbf{C}^c \nabla T\, d\Omega$
Magnetics: Induction	$F_B = \int_{\Omega} \Phi\cdot R_B\, d\Omega + \sum_e \int_{\Omega^e} \tau_B(\mathbf{R_B}\otimes\mathbf{u} - \mathbf{u}\otimes\mathbf{R_B}) : \nabla\Phi\, d\Omega + \sum_e \int_{\Omega^e} \tau_\psi(\nabla\cdot\Phi)(\nabla\cdot\mathbf{B})\, d\Omega$
Divergence Constraint	$F_\Psi = \int_{\Omega} \Phi R_\psi\, d\Omega + \sum_e \int_{\Omega^e} \tau_B \nabla\phi\cdot\mathbf{R_B}\, d\Omega$ $\sum_e \int_{\Omega^e} \tau_B \nabla\Phi\cdot[\frac{\partial\mathbf{B}}{\partial t} + \nabla\cdot[\mathbf{u}\otimes\mathbf{B} - \mathbf{B}\otimes\mathbf{u} - \frac{\eta}{\mu_0}\left(\nabla\mathbf{B} - (\nabla\mathbf{B})^T\right)] + \nabla\psi] d\Omega$

Sandia National Laboratories

Why Newton-Krylov Methods?

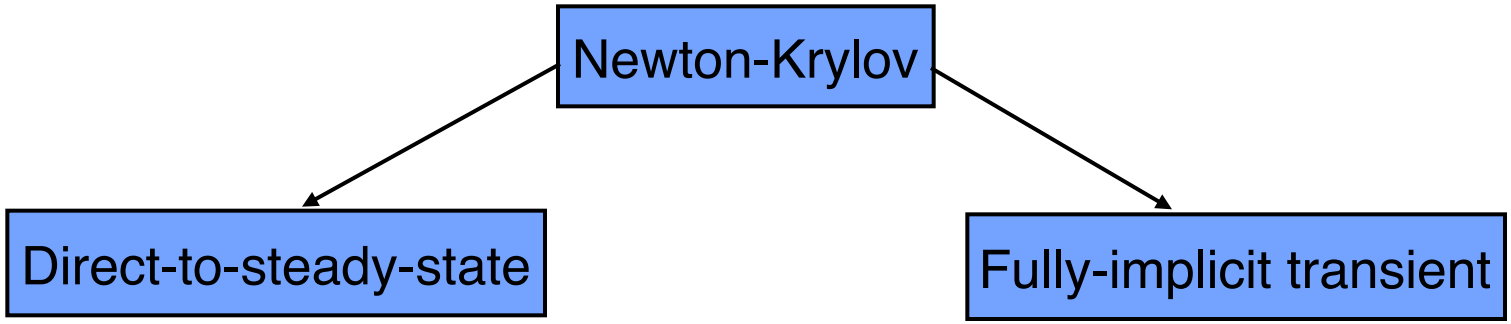

Robustness, Convergence and Flexibility

- **Strongly coupled multi-physics often requires a strongly coupled nonlinear solver**
- **Quadratic convergence near solutions**
- **Enables continuation, bifurcation, stability analysis, etc.**

Stability, Accuracy and Efficiency

- **Stable (stiff systems)**
- **High order methods**
- **Variable order techniques with error-control**
- **Can be stable, accurate and efficient run at the dynamical time-scale of interest in multiple-time-scale systems** (See e.g. Knoll et. al., Brown & Woodward., Chacon and Knoll, S. and Ober, S. and Ropp)

Sandia National Laboratories

Why Newton-Krylov Methods?

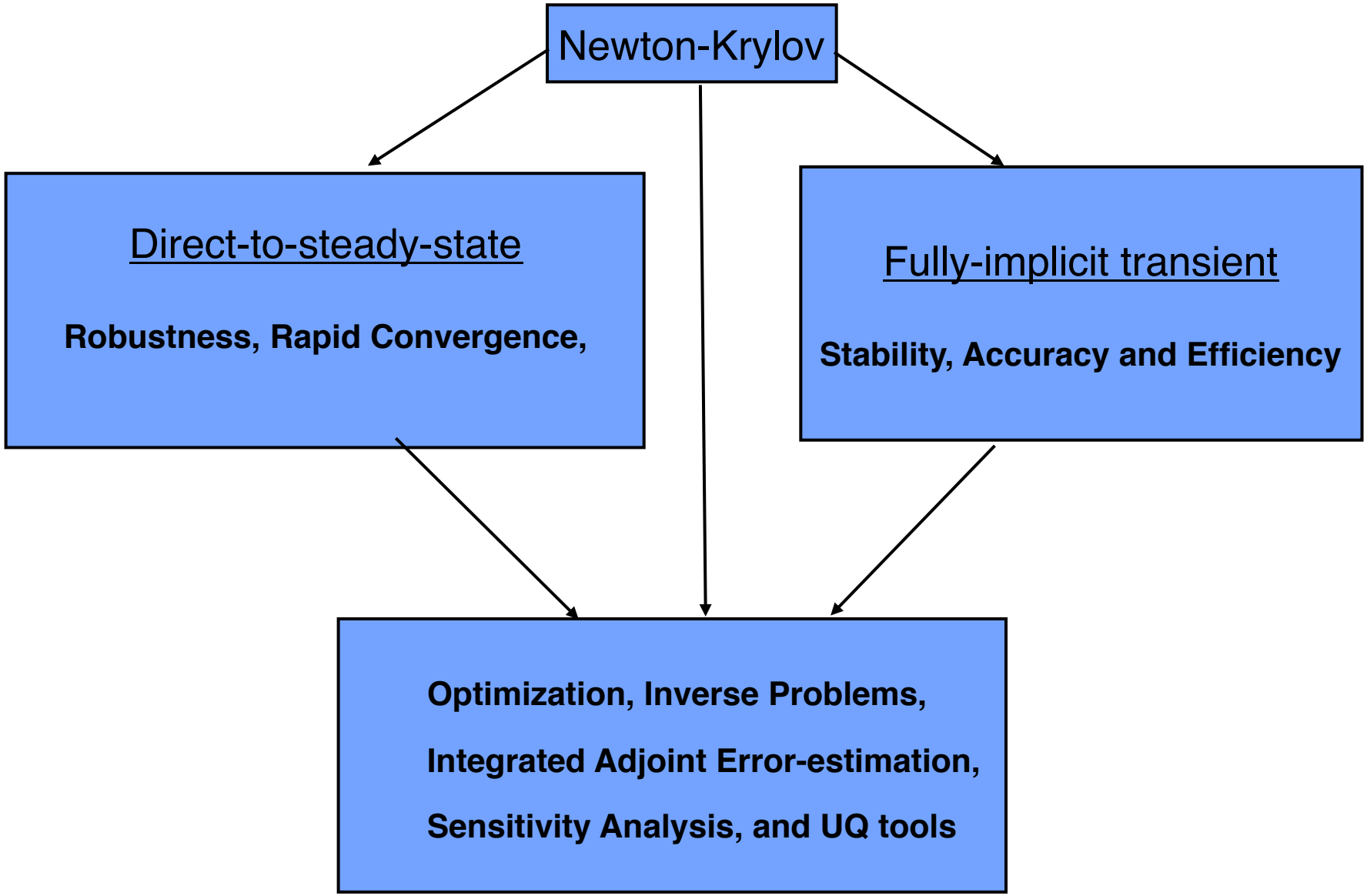

Sandia National Laboratories

Equations of State (& e.g. HydroMagnetic Thermal Cavity)

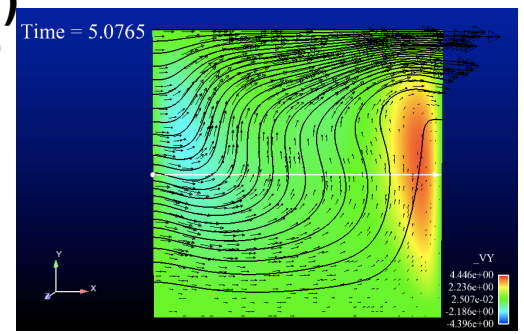

Constant Density - Strictly incompressible

$$\rho = \rho_0 = \text{ constant}$$

Boussinesq Approximation

$$\rho \approx \rho_0 + \frac{\partial \rho}{\partial T}\Big|_0 (T - T_0) \text{ in momentum body force term}$$

$$\rho = \rho_0 \text{ and everywhere else}$$

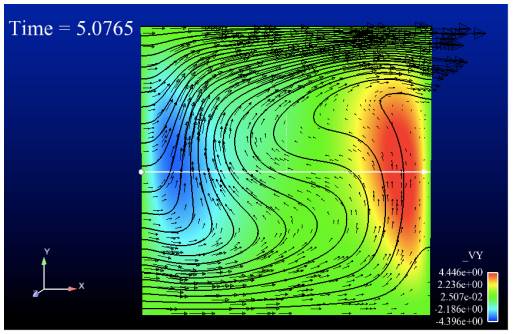

Variable density Formulations

Low Flow Mach Number Approximation

$$P_{th} = f(\rho, T, Y_i) \text{ where } P_{th} \text{ is thermodynamic not hydrodynamic pressure (P)}$$

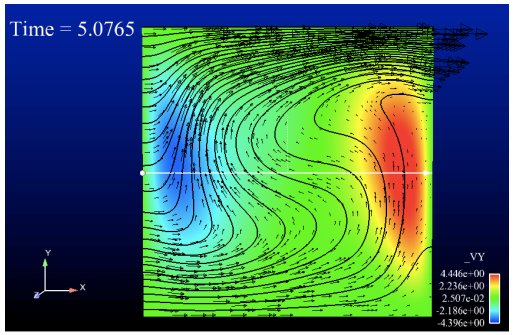

Anelastic Approximation

$$P = f(\rho, T, Y_i) \text{ and } \frac{\partial \rho}{\partial t} = 0 \text{ in continuity eq.}$$

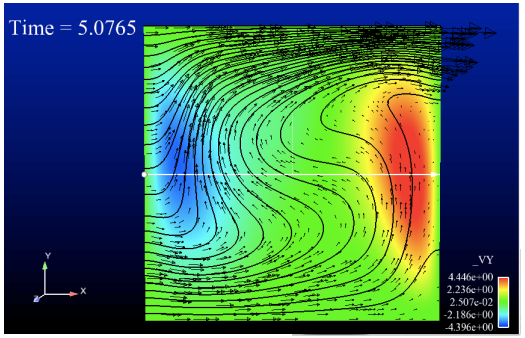

Compressible Fluid

$$P = f(\rho, T, Y_i)$$

The path to predictive computational analysis and uncertainty quantification (UQ) for multiphysics has many open challenges

Challenges Include:

- **Uncertainties arise from: discretization errors, boundary and initial conditions, model parameters, physical parameters,**
- **Analysis and design often focus on a set of quantities of interest (QoI) rather than the entire state (e.g. partial differential equation (PDE) solution)**
- **The stability, error, uncertainty propagation and sensitivity characteristics for QoI can be significantly different from the PDE solution itself**

We are addressing these challenges for studies of a moderate number of QoIs dependent on a large-number of parameters using adjoint-based methods to accurately and efficiently compute numerical error estimates and to conduct sensitivity analysis for QoI

Adjoint methods have been well studied and demonstrated for parabolic PDEs.
[e.g. Rannacher, Oden, C. Johnson, Estep, Bangerth, Barth, Suli, Braack, …..]

Forward problem: $\mathcal{L}(u;\mathrm{p}) = f(\mathrm{p})$ Adjoint problem: $(\mathcal{L}'(u;\mathrm{p}))^{*}\psi = \partial_u g(u,\mathrm{p}).$

Adjoint Sensitivities: $\partial_p g(U;p) = (\psi, \partial_p \mathcal{R}(u;p));$ Error Estimate: $g(u;p) - g(U;p) \approx (\psi, \mathcal{R}(u;p))$

Initial Adjoint Error Estimate for Resistive MHD:

Analytic Hartmann Flow (Re = , Rem = , Ha =)

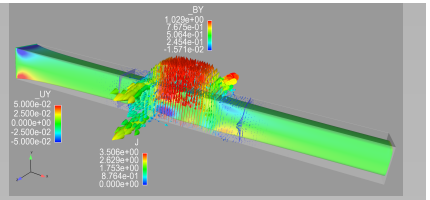

- **QoI (1) Flow: Average Fluid velocity (Vx)** $\bar{V} = \int_{-1}^{1} V_x dy$

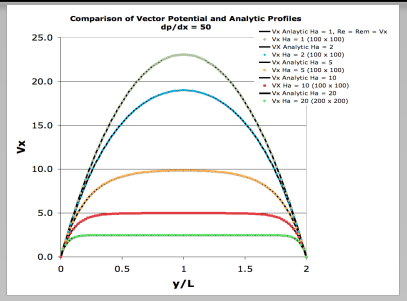

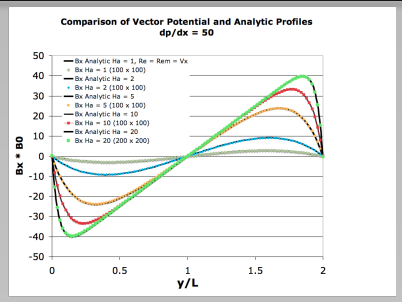

- **QoI (2) Magnetics: Average of induced field in streamwise direction (Bx)** $\bar{B}_x = \int_{0}^{1} B_x dy$

$$v_x = -\frac{\rho G_0 Ha}{\mu_0 B_0^2}\left[\frac{\cosh(Ha) - \cosh(yHa/L)}{\sinh(Ha)}\right]$$

$$B_x = -\frac{B_0 Re_m}{Ha}\left[\frac{\sinh(yHa/L) - (y/L)\sinh(Ha)}{\cosh(Ha) - 1}\right]$$

$$Re = \frac{\rho V L}{\mu};\ Re_m = \frac{VL}{\eta}$$

$$Ha = \frac{B_0 L}{\sqrt{\mu\eta}}$$

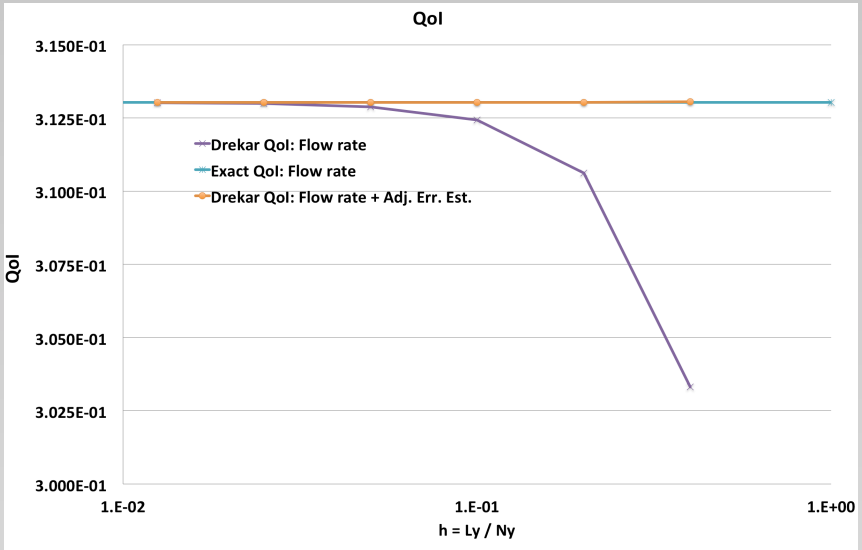

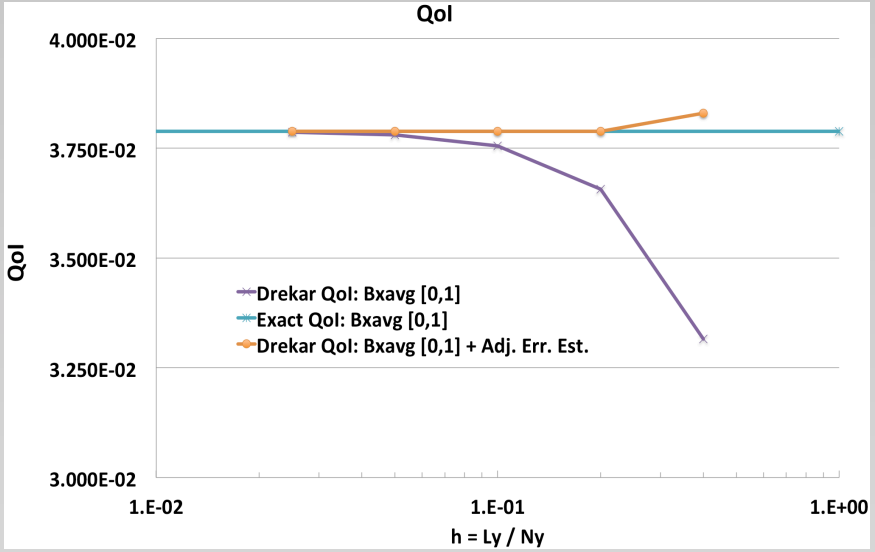

Initial Adjoint Sensitivity Analysis for Resistive MHD: MHD Duct Flows

E.g. Analytic Hartmann Flow

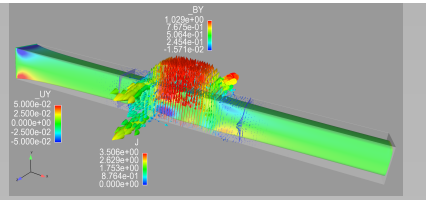

- **QoI (1) Flow: Average Fluid velocity (Vx)** $\bar{V} = \int_{-1}^{1} V_x dy$

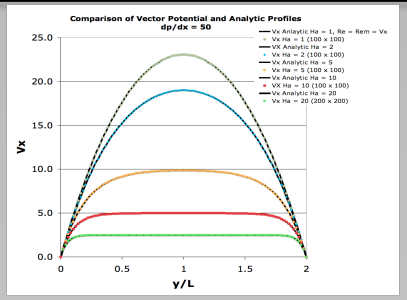

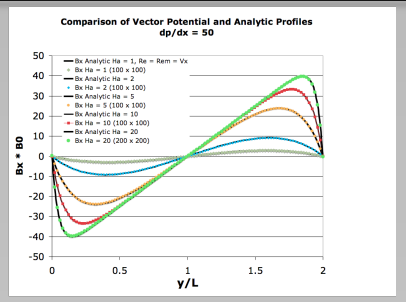

- **Base State**
  - **Ha =**

$$v_x = -\frac{\rho G_0 Ha}{\mu_0 B_0^2}\left[\frac{\cosh(Ha) - \cosh(yHa/L)}{\sinh(Ha)}\right]$$

$$B_x = -\frac{B_0 Re_m}{Ha}\left[\frac{\sinh(yHa/L) - (y/L)\sinh(Ha)}{\cosh(Ha) - 1}\right]$$

$$Re = \frac{\rho V L}{\mu};\ Re_m = \frac{VL}{\eta}$$

$$Ha = \frac{B_0 L}{\sqrt{\mu\eta}}$$

E.g. Very Coarse Mesh Simulation: 5 elements in duct cross-section

Physical Parameter	Exact Sensitivity	Computed Adjoint Sensitivity	Relative Error
Pressure Gradient (G_0)	-0.31304	-0.3148	0.6%
Dynamic Viscosity (μ)	-0.294485	-0.2858	2.9%

Initial Adjoint Sensitivity Analysis for Resistive MHD: MHD Duct Flows

E.g. 3D MHD Generator (Re = 2500, Re_m = 10, Ha = 5)

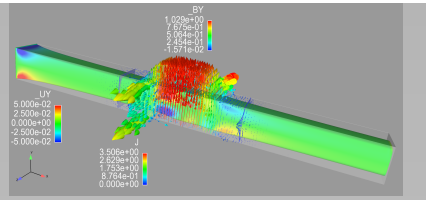

$$Re = \frac{\rho V L}{\mu}; \quad Re_m = \frac{VL}{\eta} \quad Ha = \frac{B_0 L}{\sqrt{\mu\eta}}$$

- **QoI (1) Flow: Average Fluid velocity (Vx)** $\bar{V} = \int_{-1}^{1} V_x dy$
- **Reference state:** $\rho = 1, \mu = 0.002, G_0 = 0.31, \eta = 1, B_0 = 0.2236$
- **Parameters in simple numerical sensitivity study (+- 1%, 5%) :** $\mu, G_0;$

E.g. Coarse Mesh Simulation: N_x x N_y x N_z: 140x20x20 mesh

Physical Parameter Dynamic Viscosity (μ)	QoI computed from Drekar	QoI Estimated from Adjoint Sensitivity	Relative Error
0.00202 (μ+1%)	4.61750	4.61703	0.010%
0.00198 (μ-1%)	4.69811	4.69784	0.006%
0.0021 (μ+5%)	4.46483	4.45541	0.211%
0.0019 (μ-5%)	4.86876	4.85945	0.191%

Initial Scaling Studies for Cray XK7 AND BG/Q.
3D MHD Generator [Re = 500, Re_m = 1, Ha = 2.5]

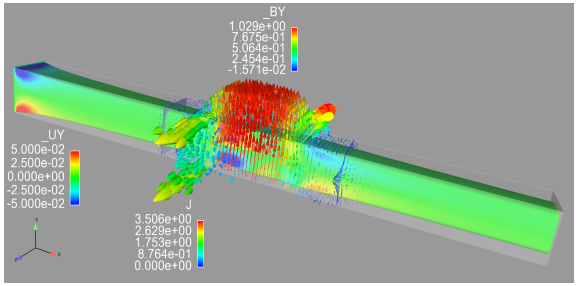

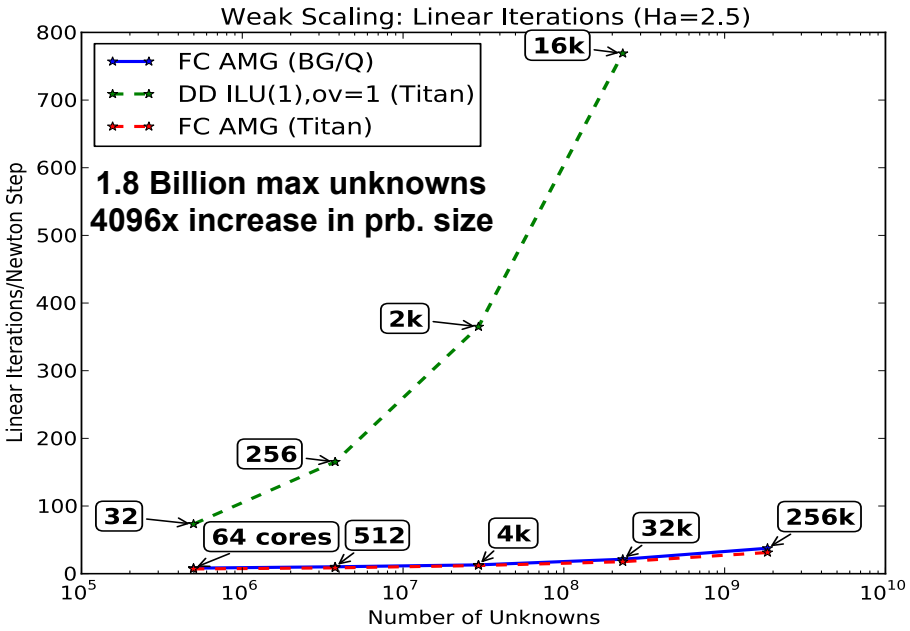

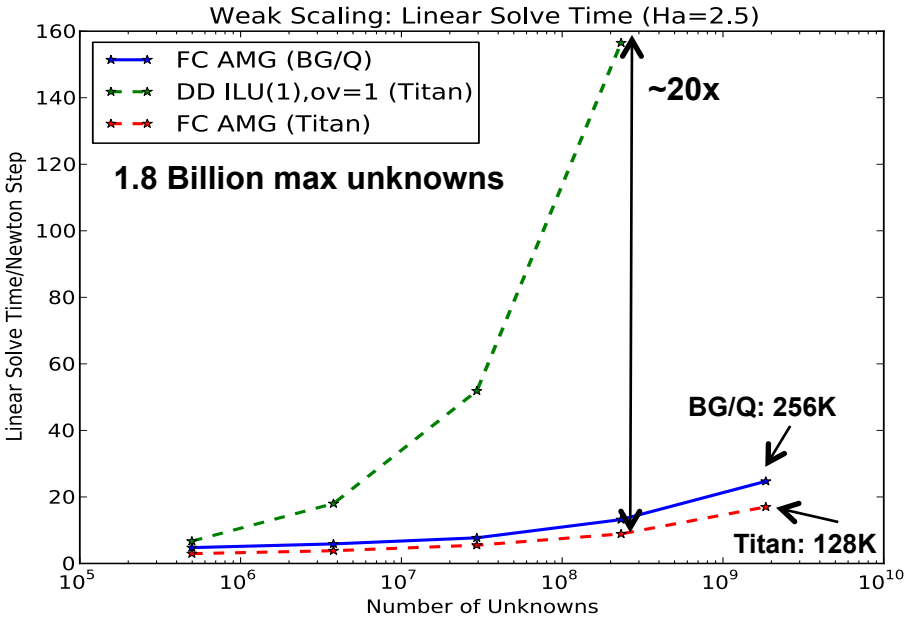

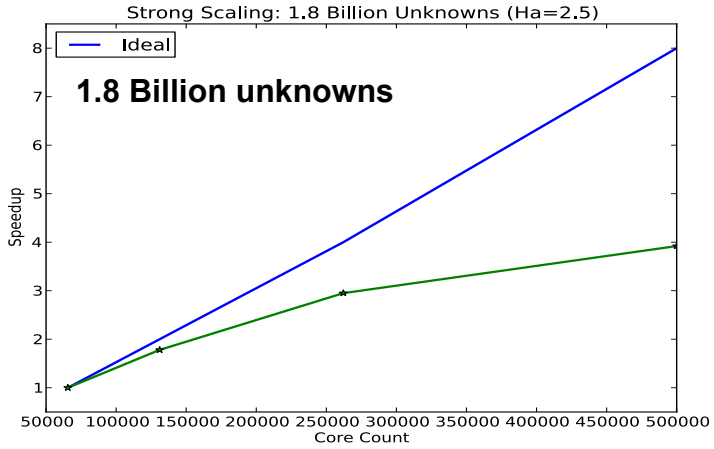

Recently run on 500,000 cores of BG/Q

[Preliminary strong scaling of Krylov linear solver + preconditioner [(ML: FC – AMG), Tuminaro, Hu, Siefert et. al.]

Sandia National Laboratories

Initial Scaling Study for Cray XK7.
3D Hydromagnetic Kelvin-Helmholtz Instability
[Re = 10^4, Re_m = 10^4, M_A = 3; CFL_{max} ~5]

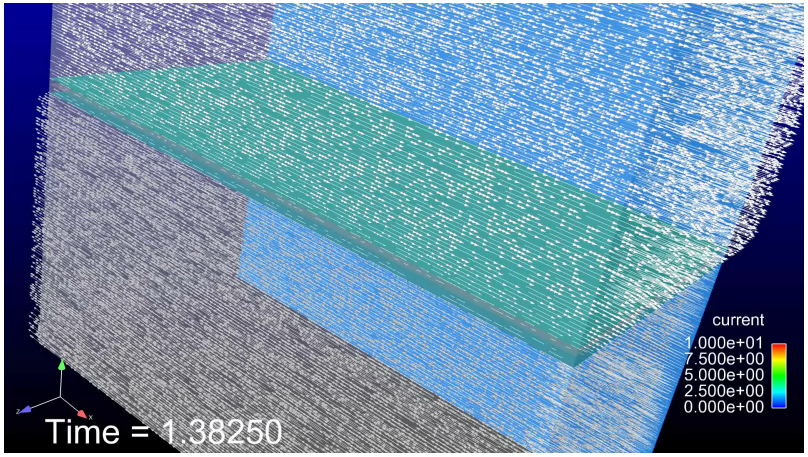

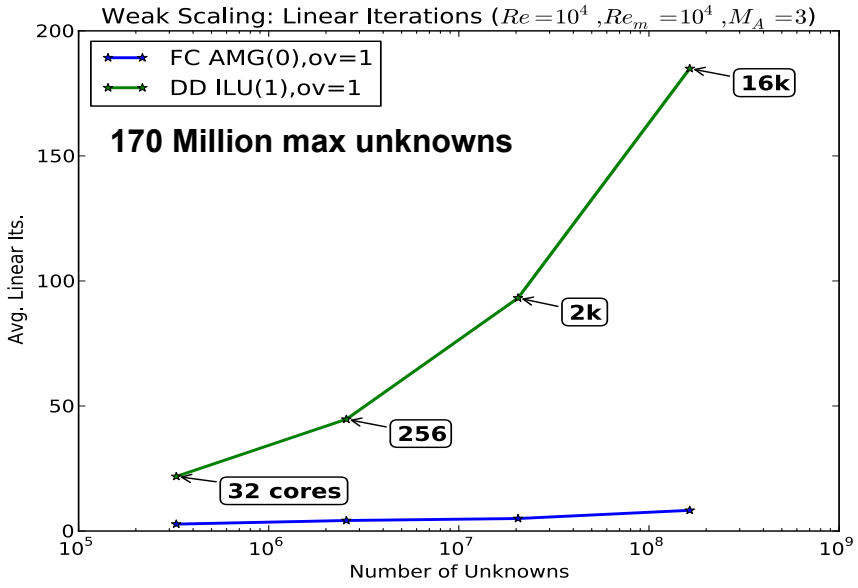

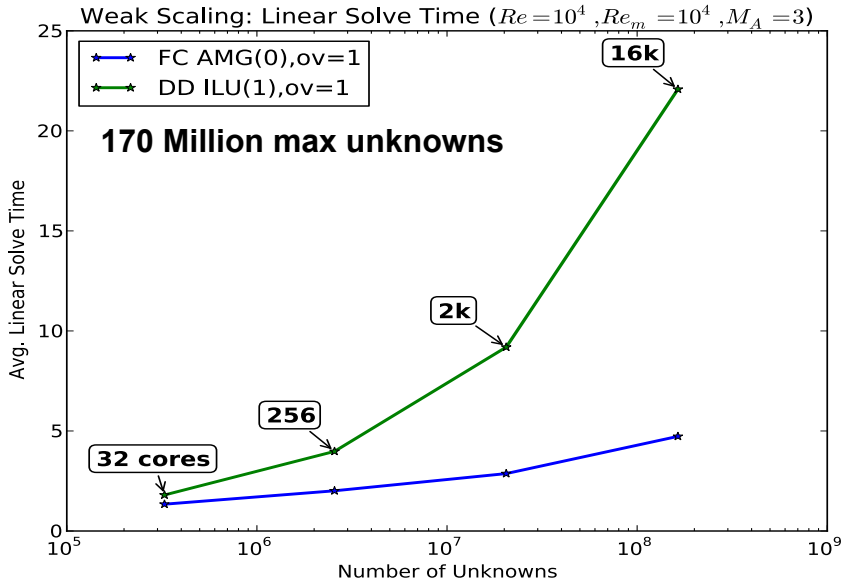

Sandia National Laboratories

Computational Physics Study: Understanding Time-scales in Magnetic Reconnection

Magnetic reconnection is a fundamental process whereby the sheared magnetic field topology is altered via some mechanism (e.g dissipation), resulting in a rapid conversion of magnetic field energy into plasma energy and significant plasma transport.

Magnetic reconnection dominates the energetics and dynamics of most space and laboratory plasmas.

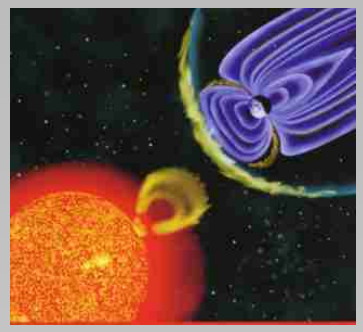

Magnetosphere
Credit: Steele Hill/NASA

Astrophysics
- Solar Flares,
- coronal mass ejections,
- plasmoid ejection from earth's magnetotail.

Magnetic Confined Fusion Devices (e.g. ITER)
- Break of plasma confinement (e.g. Sawtooth crash),
- resulting huge energy loss,
- and discharge of very large electrical currents into walls of structure.

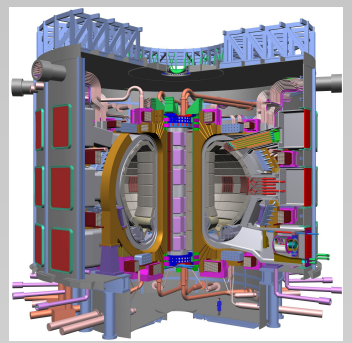

ITER

ITER can sustain a limited number of disruptions, O(10 – 100). [FSP Report]

However, plasmas in all the above-mentioned cases are known to have a negligible resistivity that cannot be used to explain the reconnection time-scales observed. This issue has drawn significant attention over the last 50 years. [See e.g. D. Biskamp, Magnetic Reconnection in Plasmas. 2000]

Multiple-time-scale systems: E.g. Driven Magnetic Reconnection with a Magnetic Island Coalescence Problem (Incompressible)

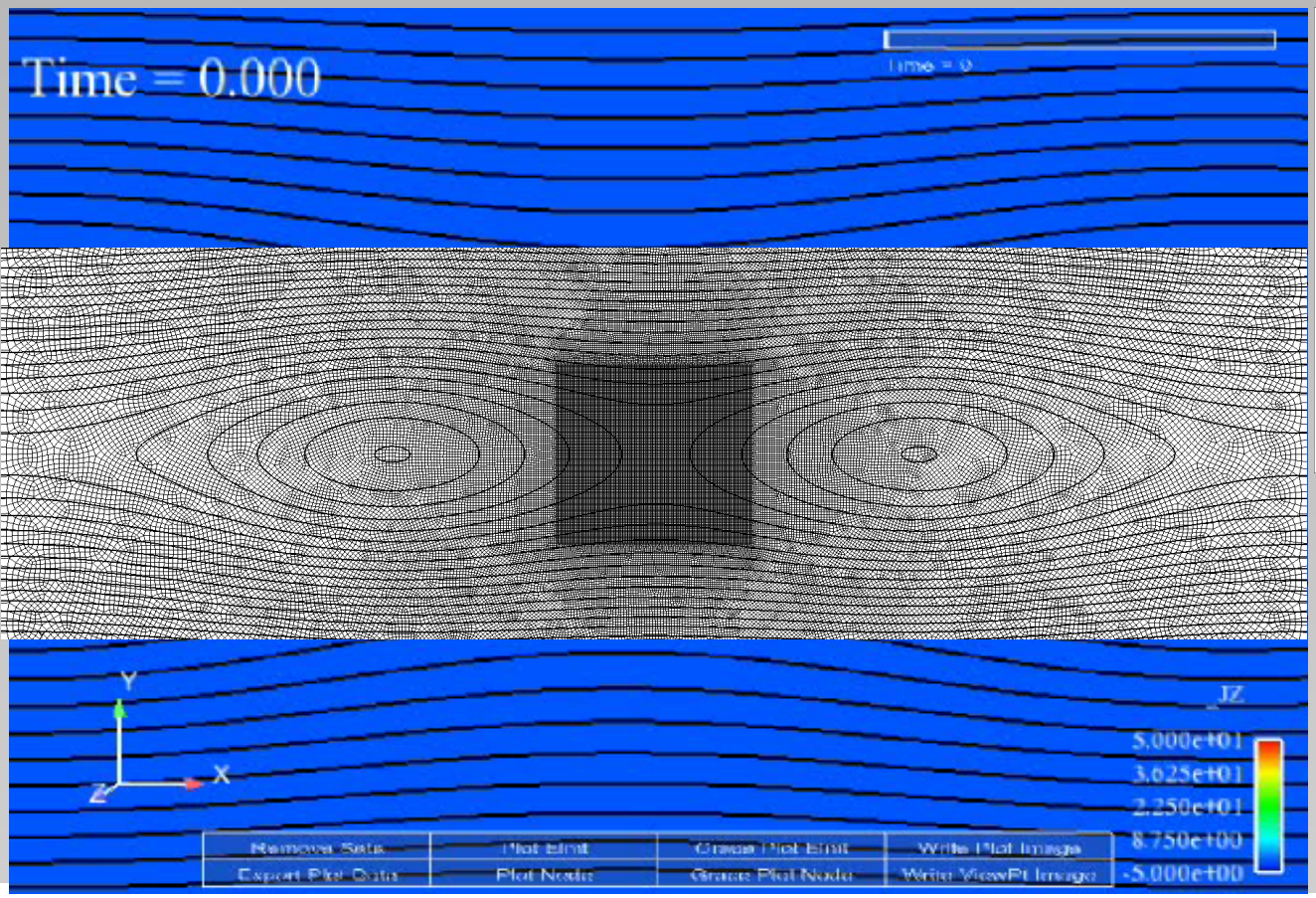

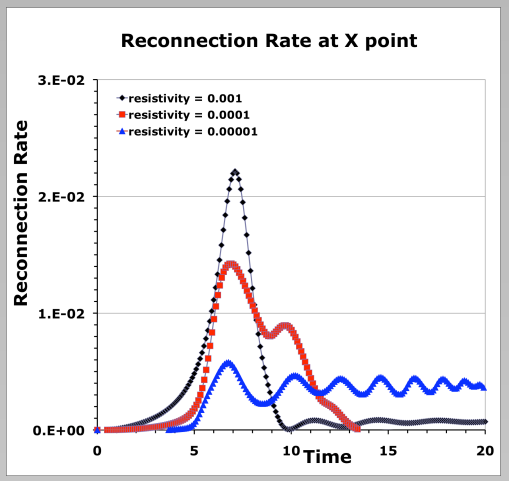

Approx. Computational Time Scales:

- **Ion Momentum Diffusion: 10^{-7} to 10^{-3}**
- **Magnetic Flux Diffusion: 10^{-7} to 10^{-3}**

- **Ion Momentum Advection: 10^{-4} to 10^{-2}**
- **Alfven Wave $\left(\tau_A = \frac{h\sqrt{\rho\mu_0}}{B_O}\right)$: 10^{-4} to 10^{-2}**
- **Whistler Wave $\left(\tau_w = \frac{h^2}{V_A d_i}\right)$: 10^{-7} to 10^{-1}**
- **Magnetic Island Sloshing: 10^{0}**
- **Magnetic Island Merging: 10^{1}**

[Finn and Kaw, 1977; Chacon and Knoll, 2006]

Global system level view of reconnection rate in the IC problem

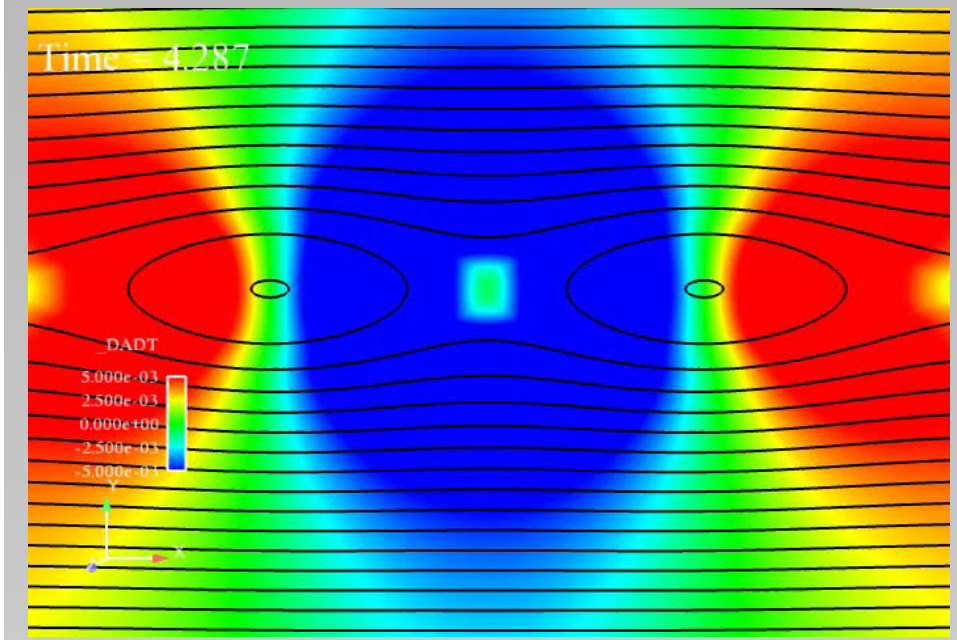

S = 1e+4

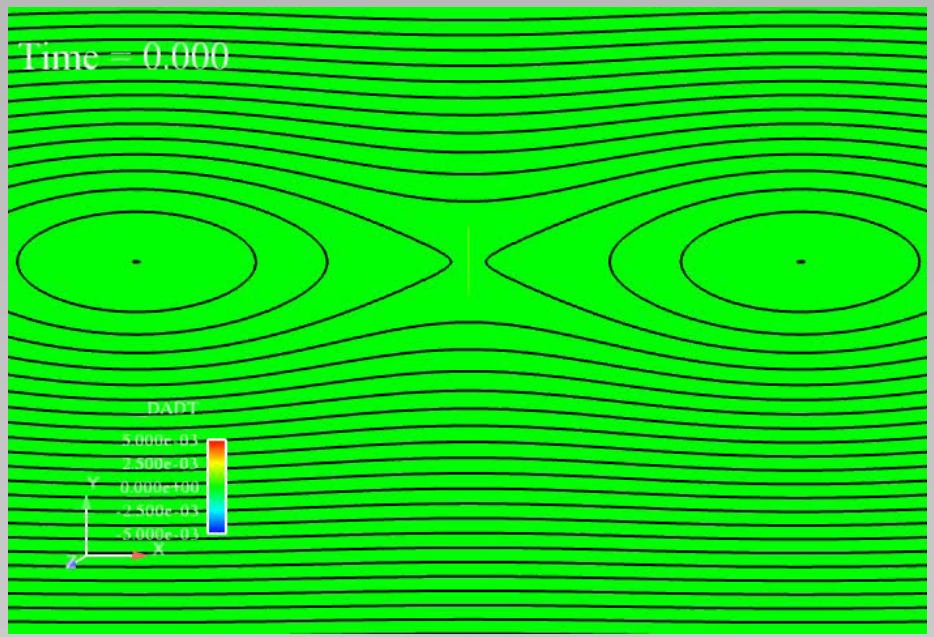

S = 1e+9

Recent insight into breakdown of thin current sheets:

Linear Theory - Asymptotic anal., Super-Alfvénic tearing instability: N. F. Loureiro et al., Phys. Plas. 2007

MHD Numerical Confirmation (idealized system, $S <= 10^8$): Samtaney et.al., Phys. Rev. L. 2009

MHD Numerical Investigations Quadra-pole system: Bhattacharjee ($10^4 < S < 6 \times 10^5$), Phys. Plas. 2009

Fully Kinetic Simulations: Daughton et. al. Phys. Rev. L. 2009

$S = 10^9$ (no claim this is effective S yet)

S = 1e+4

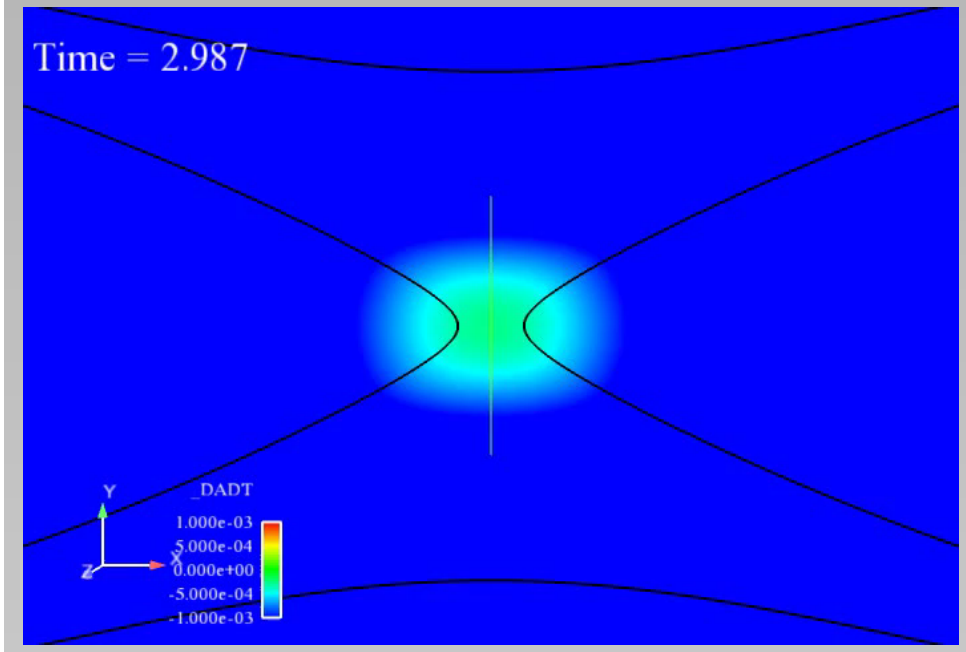

S = 1e+6

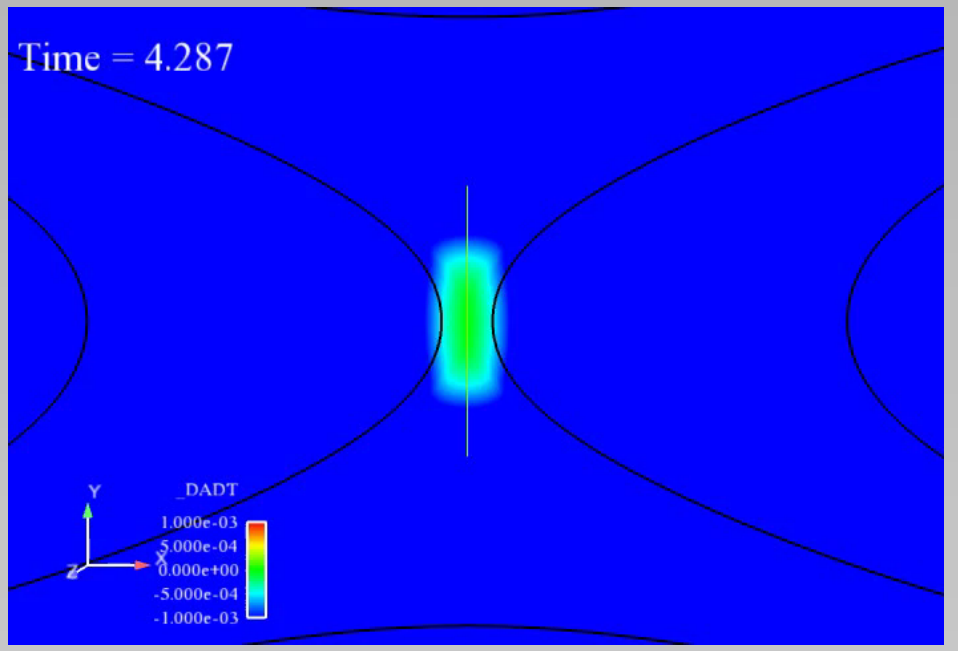

S = 1e+7

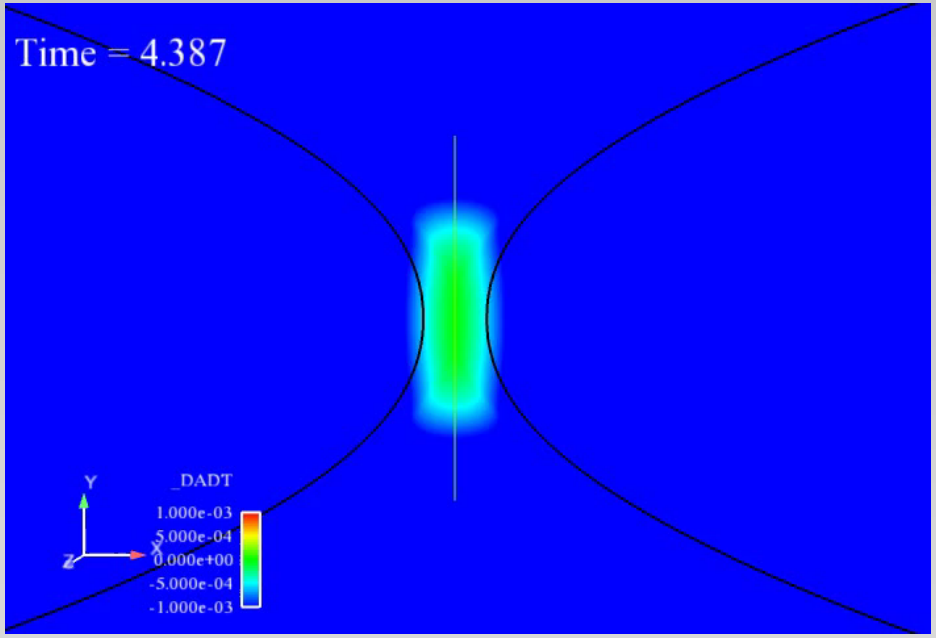

S = 1e+10

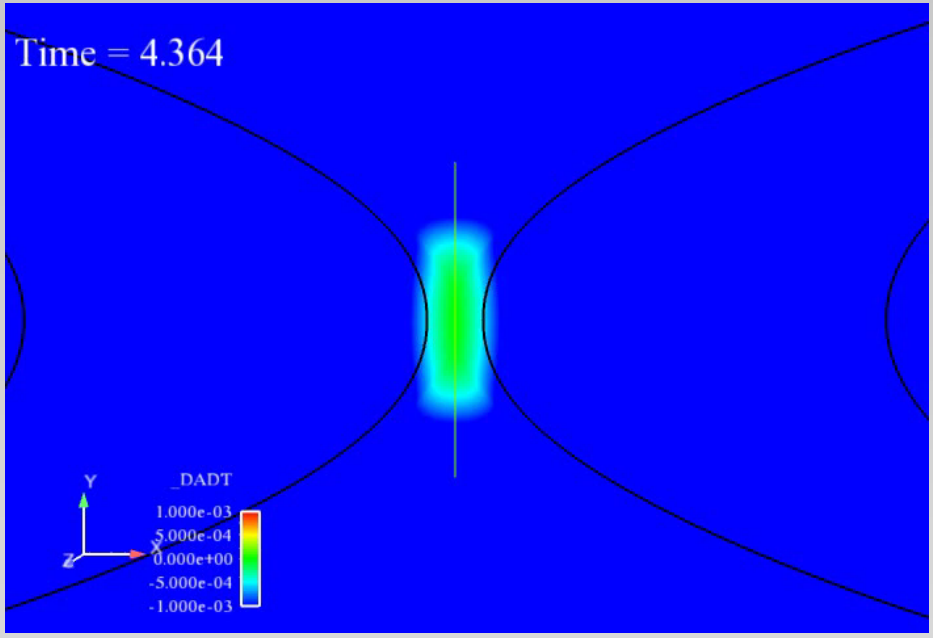

Results (Preliminary)– High Lundquist No. Reconn.: Secondary Plasmoid Instability

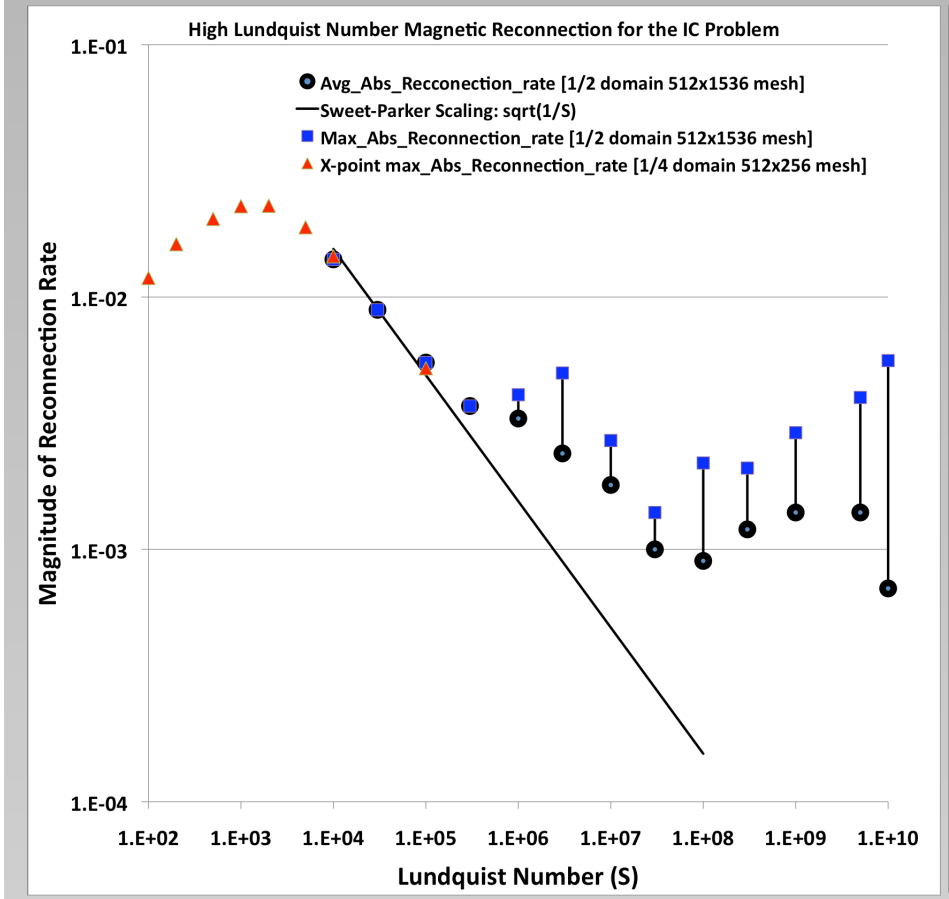

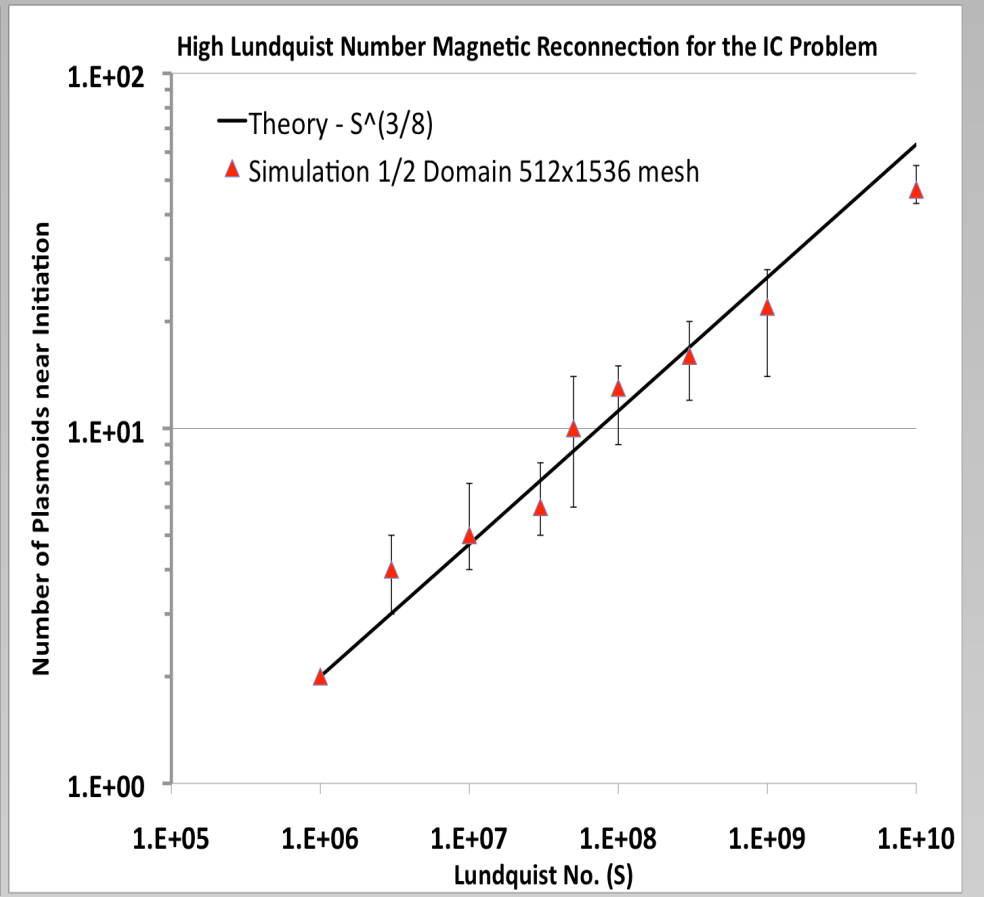

Recent insight into breakdown of thin current sheets:

Linear Theory - Asymptotic anal., Super-Alfvénic tearing instability: N. F. Loureiro et al., Phys. Plas. 2007

MHD Numerical Confirmation (idealized system, $S <= 10^8$): Samtaney et.al., Phys. Rev. L. 2009

MHD Numerical Investigations Quadra-pole system: Bhattacharjee ($10^4 < S < 6 \times 10^5$), Phys. Plas. 2009

Fully Kinetic Simulations: Daughton et. al. Phys. Rev. L. 2009

Geodynamo Mechanisms
Geodynamo Slides from J. Aurnou Talk (UCLA – Earth and Space Sciences Dept.)

Necessary Ingredients

- A dynamo requires:
  1. An electrically-conducting material
  2. A sufficiently large body of material
  3. An energy source to drive motions of the material
  4. (Some net organization of the motions)

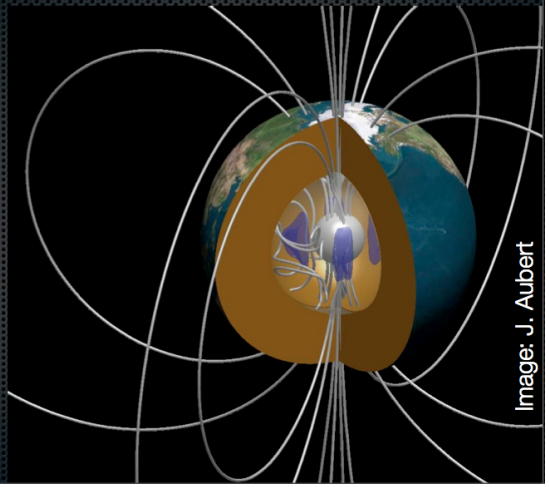

Where is the Field Generated?

- Crust has some magnetic materials
  - Cannot explain observed temporal variability
- Mantle is non-magnetic (too hot) & electrically insulating
- Core dynamo
  - Planetary dynamo converts Earth's internal energy into magnetic field energy
  - Re_m ~ 10^2 to 10^3

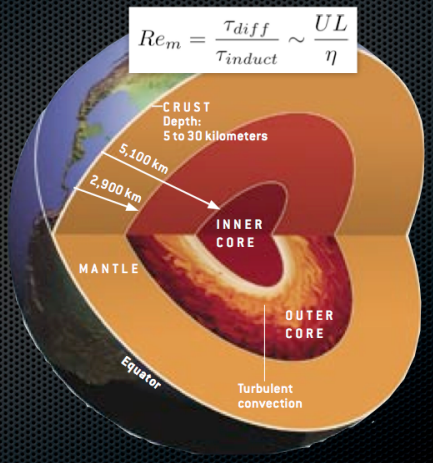

Image: Glatzmaier & Olson *Sci Am* 05

Why is the Field Nearly Axial?

- Time averaged dipole field is closely aligned along the rotation axis
  - Geocentric axial dipole (GAD) hypothesis
- Axial alignment likely due to the aligned flows that generate it

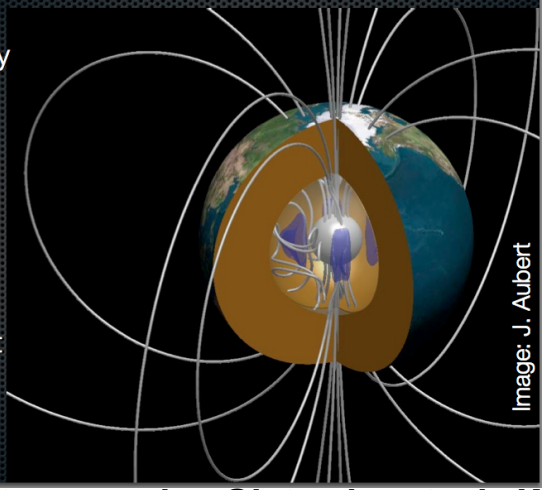

Why is the Field Nearly Axial?

- In rapidly rotating systems, flows tend to align along the rotation axis
- Long-lived idea:
  - Rotationally-controlled flows explain planetary observations

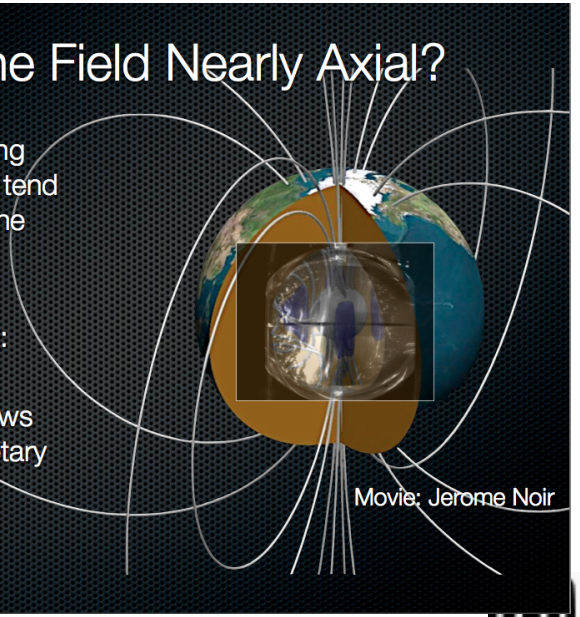

See e.g. Christensen. al., , Glatzmier et. al., Wicht et. al.

Sandia National Laboratories

Table 1. Typical Nondimensional Parameters Used in Boussinesq Dynamo Models, With Comparative Estimates for Earth's Core[a]

Term	Explanation	Definition	Earth's Core	Dynamo Factory Models	Dynamo Subset
Ra	buoyancy/diffusion	$\alpha_T g_o \Delta T L^3/\nu\kappa$	$\sim 2 \times 10^{24}$	$3 \times 10^5 \leq Ra \leq 2.2 \times 10^9$	$2 \times 10^6 < Ra < 5 \times 10^8$
E	Coriolis/viscosity	$\nu/2\Omega L^2$	$\sim 10^{-15}$	$5 \times 10^{-7} \leq E \leq 5 \times 10^{-4}$	$5 \times 10^{-6} \leq E \leq 10^{-4}$
Pr	viscous diffusion/thermal diffusion	ν/κ	$\sim 10^{-1}$	$0.1 \leq Pr \leq 30$	$1 \leq Pr \leq 2$
Pm	viscous diffusion/magnetic diffusion	ν/η	$\sim 10^{-6}$	$0.06 \leq Pm \leq 20$	$1 \leq Pm \leq 2$
χ	radius ratio	R_i/R_o	0.35	0.35	0.40
Nu	total heat flux/conductive heat flux	$qL/k\Delta T$	$\sim 5 \times 10^4$	$1 < Nu < 32$	$2.5 < Nu < 25$
Λ	Lorentz/Coriolis	$\sigma B_o^2/2\rho\Omega$	$\sim 10^{-1}$	$0.013 < \Lambda < 150$	$0.14 < \Lambda < 42$
Ra_t	boundary layer crossing	$E^{-7/4}$	$Ra/Ra_t \approx 2 \times 10^{-2}$	$0.013 < Ra/Ra_t < 40$	$0.042 \leq Ra/Ra_t \leq 42$
Re	inertia/viscosity	UL/ν	$\sim 10^8$	$1 < Re < 3 \times 10^3$	$30 < Re < 3 \times 10^3$

From: King, Soderlund, Christensen, Wicht, Auronu, "Convective heat transfer in planetary dynamos", Geochemistry. Geophysics, and Geosystems (2010)

Sandia National Laboratories

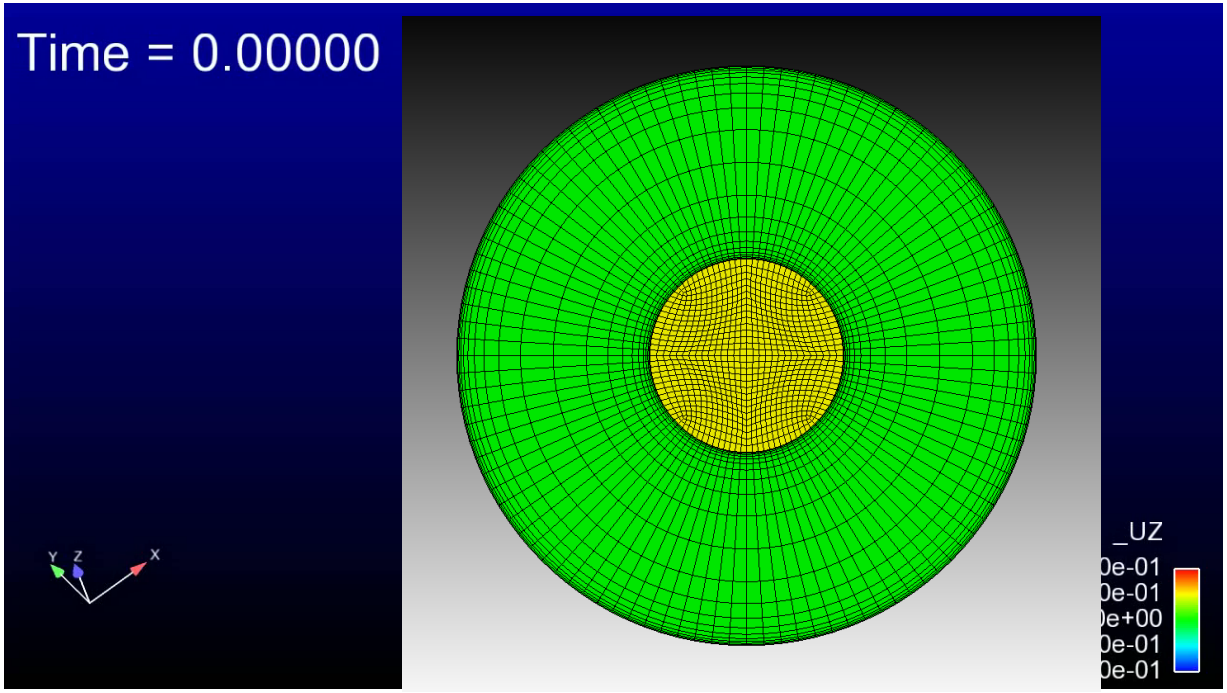

Christensen et. al.
Rotating Thermal Conv.
Benchmark
Ra = 1e5, E = 1e-3;

E_kin = 58.348 +- 0.050

Preliminary
Drekar 1.3M elem. Soln.

E_kin = 58.846
This is within .85%

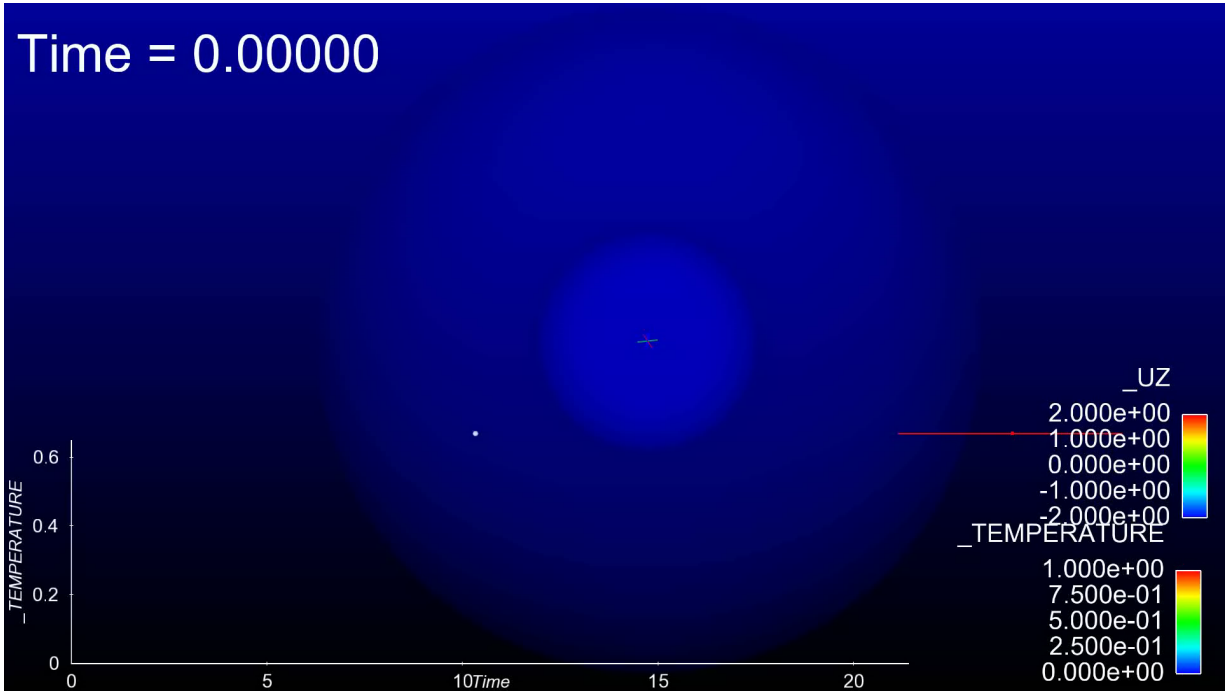

Ra = 1.54e5, E = 1e-3;

Sandia National Laboratories

J. Aurnou - Spin Laboratory (UCLA – Earth and Space Sciences Dept.)

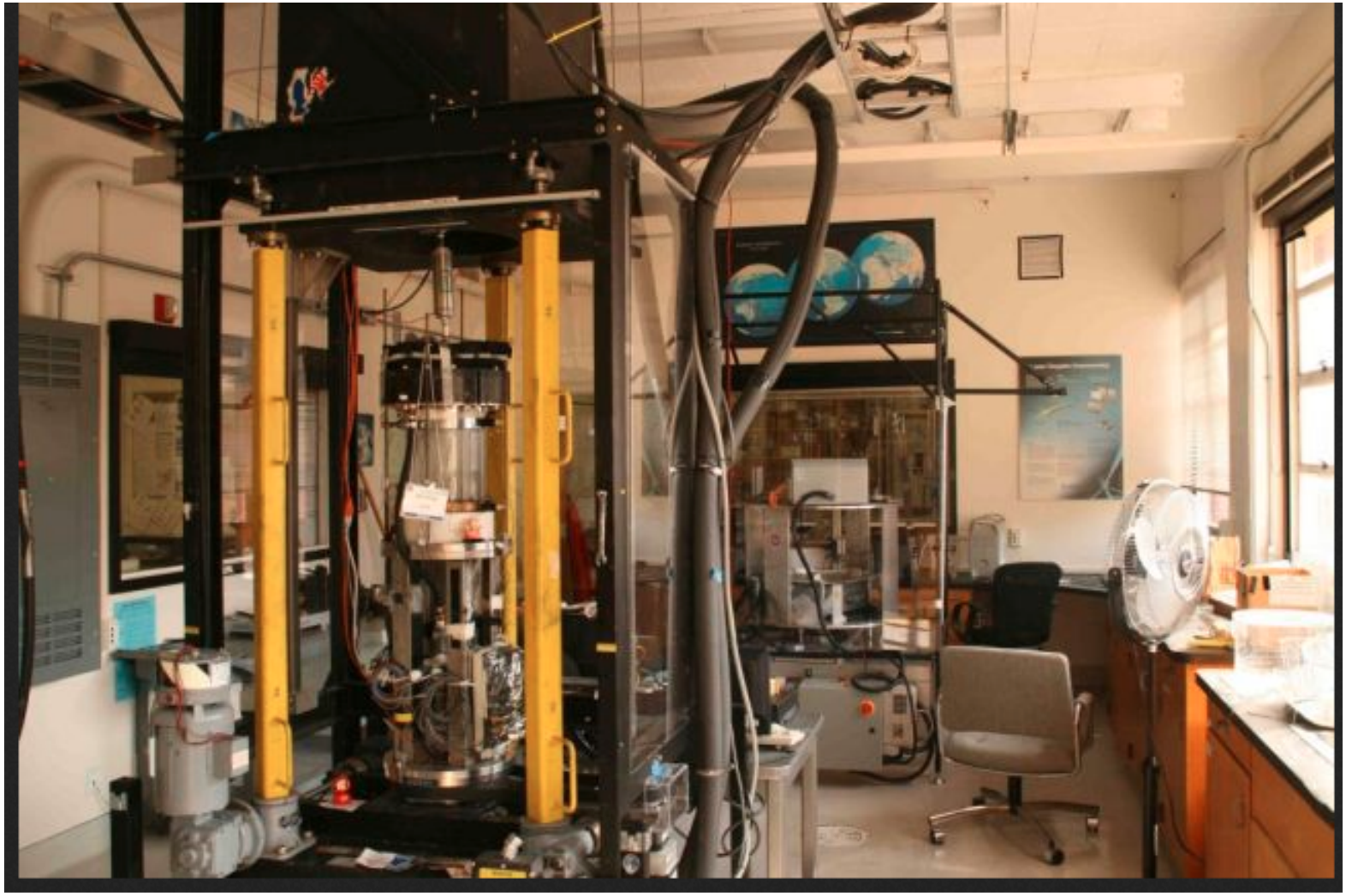

Sandia National Laboratories

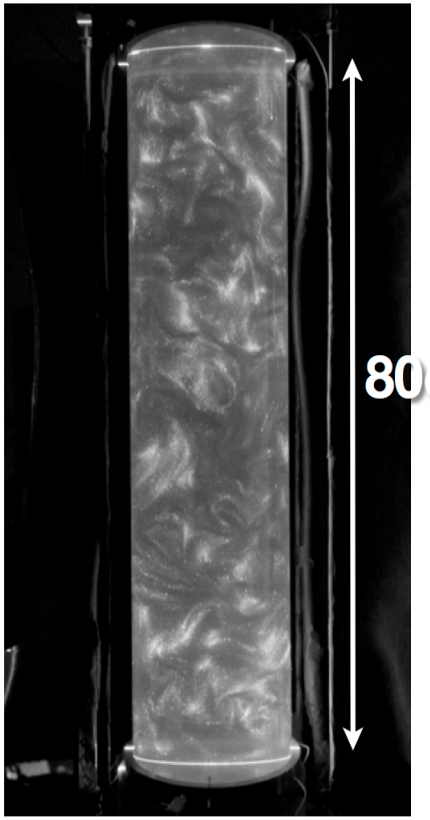

Ra~ 3e10

Aurnou et. al.
Lab Exp.

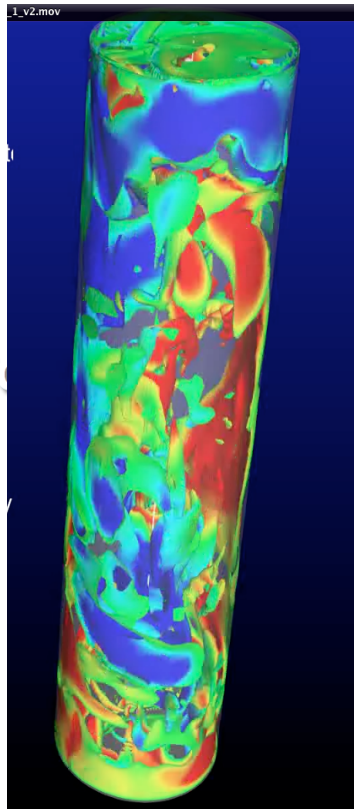

Ra = 1e10

Preliminary Drekar
Simulation

Ra~ 6e10; E ~1e-7

Aurnou et. al.
Lab Exp.

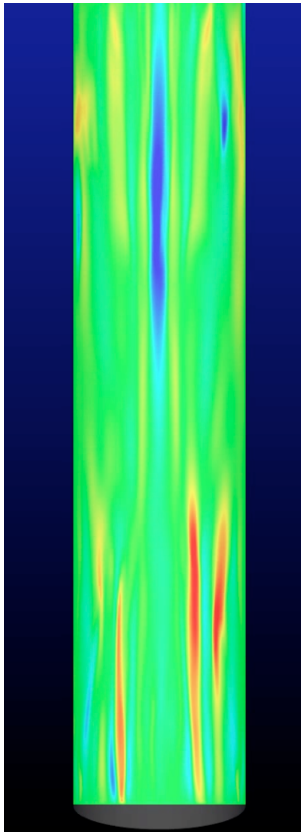

Ra = 1e11; E = 2e-7

Preliminary Drekar
Simulation

Sandia National Laboratories

Ra = 1e11;
E = 0

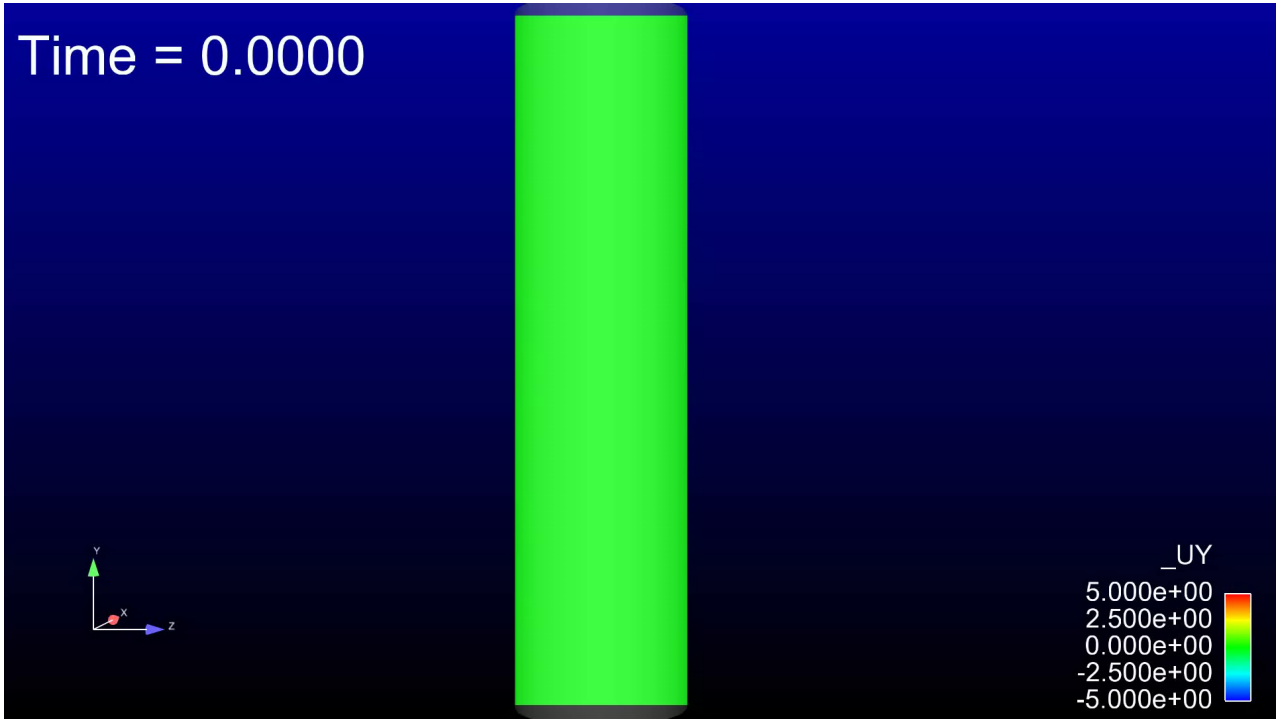

Ra = 1e11;
E = 2e-7

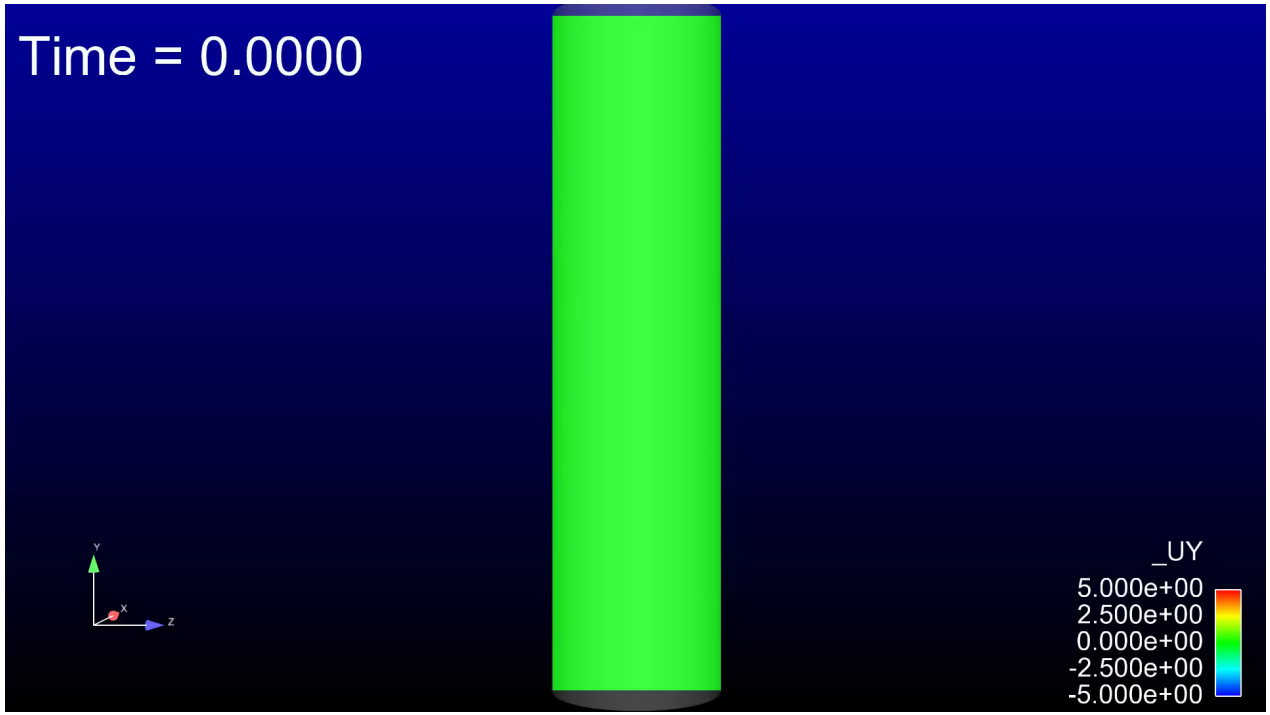

Sandia National Laboratories

Ra = 1e11;
E = 0

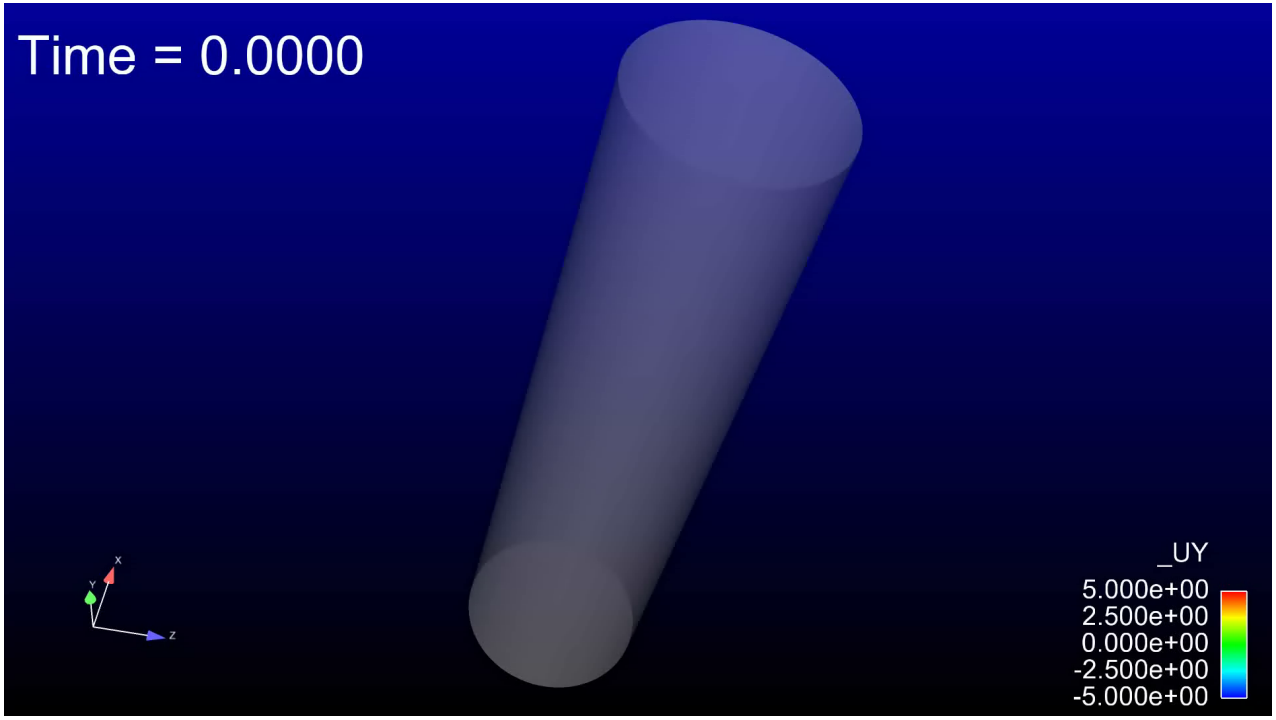

Ra = 1e11;
E = 2e-7

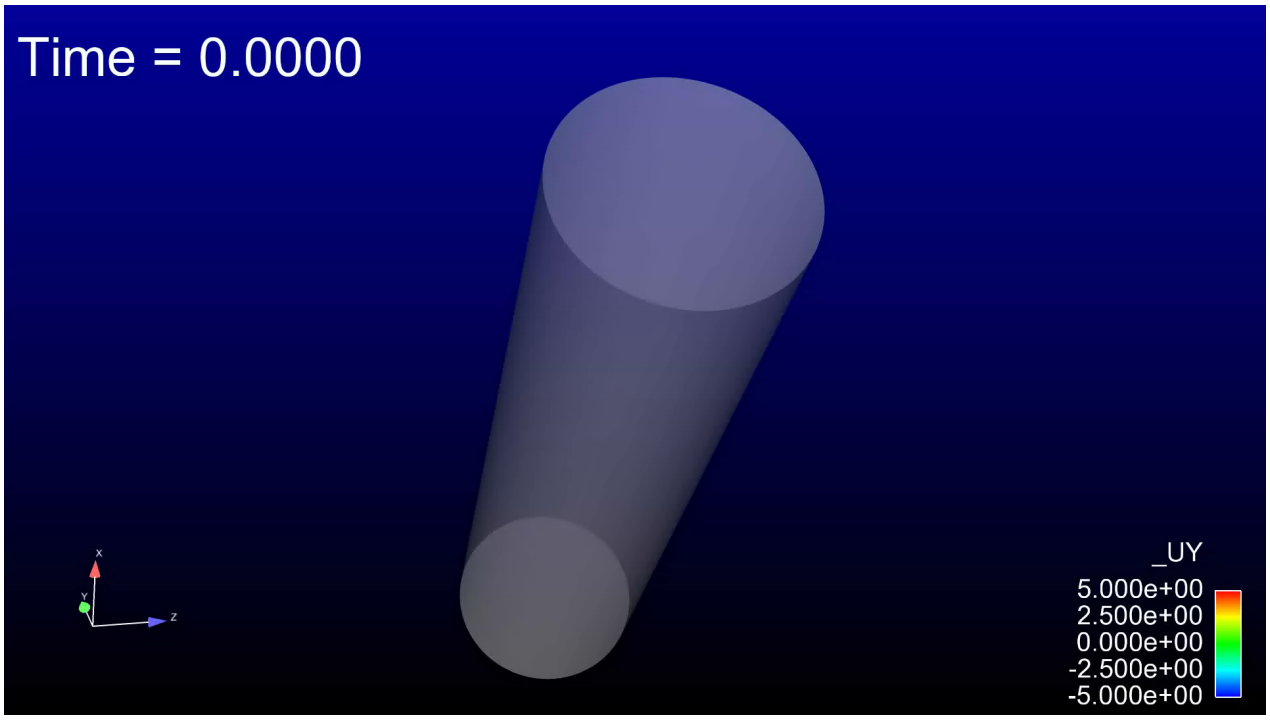

Sandia National Laboratories

Preliminary Comparison Non-rotating Thermal Convection Experiments and Drekar (E = 0, Pr = 7.1)

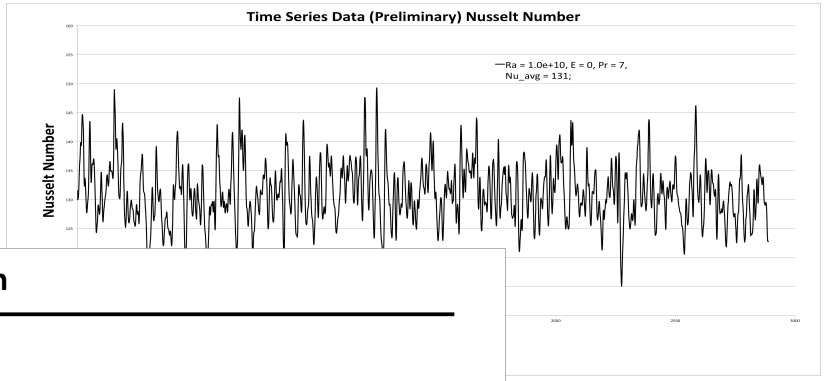

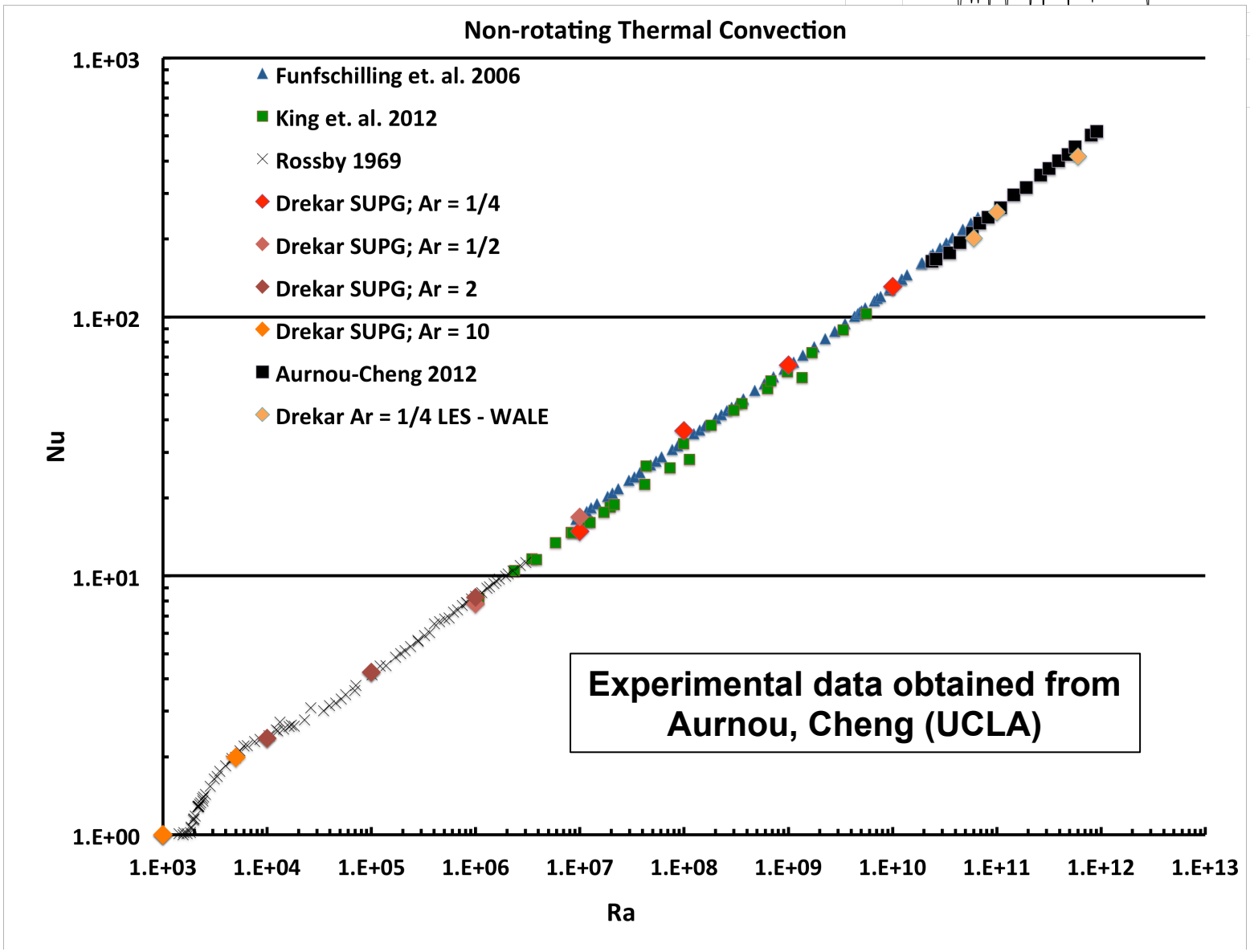

Sandia National Laboratories

MHD Turbulence Modeling
Taylor–Green MHD Vortex Decay: Re = 5100 (Drekar FE VMS Resistive MHD Model)

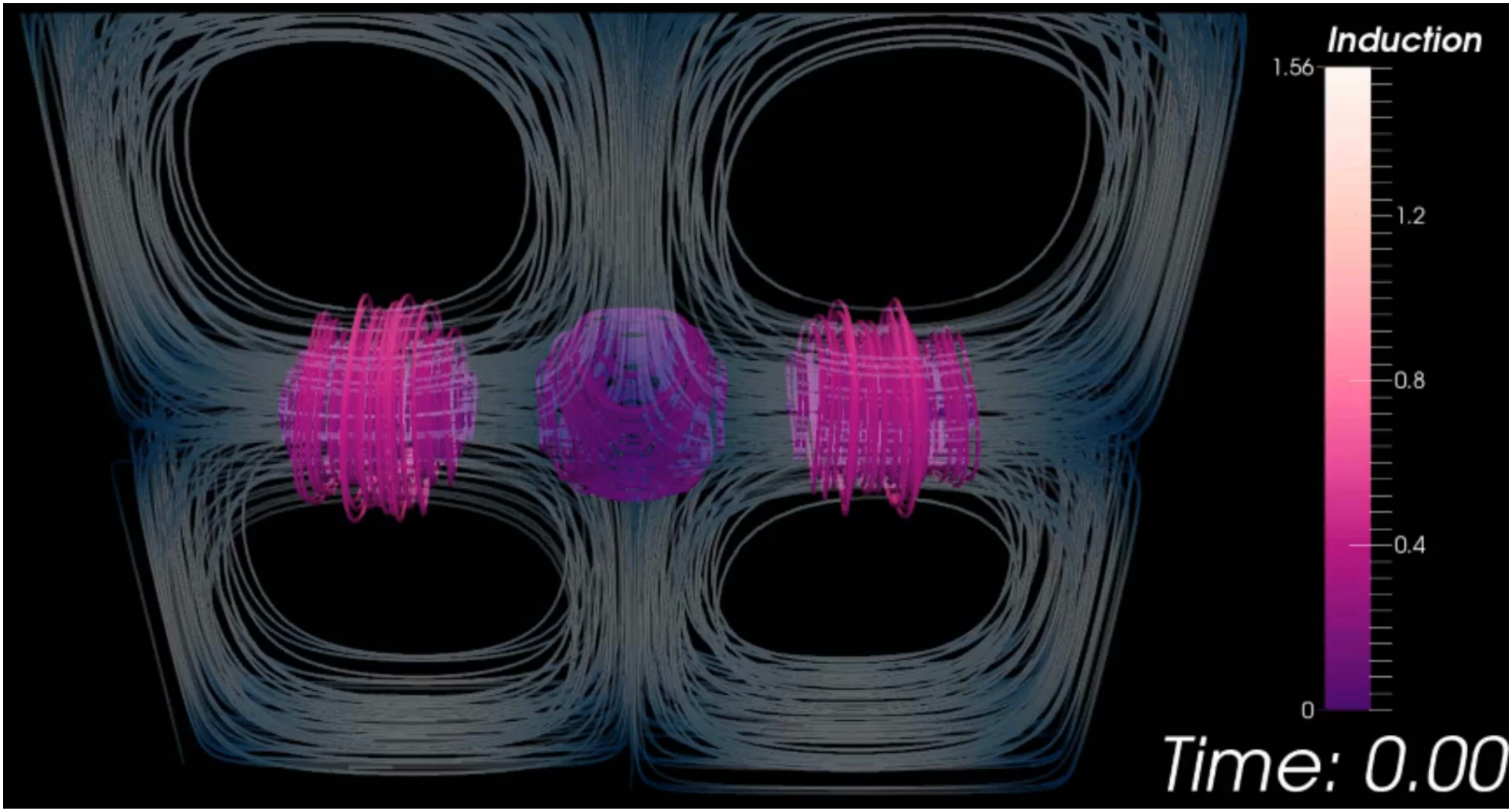

With:
Prof. Assad Oberai (RPI),
David Sondak (DOE Office of Science Graduate Fellowshiand recent Ph. D. – RPI)

Sandia National Laboratories

Following Variational Multiscale Method (Hughes et. al.) develop FE VMS MHD model

With Assad Oberai, David Sondak (RPI)

Find $\mathbf{U}^h \in \mathcal{V}^h$ *s.t.*

$$\mathcal{A}\left(\mathbf{W}^h, \mathbf{U}^h + \mathbf{U}'\right) = \left(\mathbf{w}^h, \mathbf{f}^{\mathrm{V}}\right) + \left(\mathbf{v}^h, \mathbf{f}^{\mathrm{I}}\right) \qquad \forall\, \mathbf{W}^h \in \mathcal{V}^h.$$

$$\mathbf{U}' \approx -\mathbb{P}'\left[\boldsymbol{\tau}\mathbb{P}'^{T}\left[\boldsymbol{\mathcal{R}}\left(\mathbf{U}^h\right)\right]\right].$$

$$\boldsymbol{\mathcal{R}}\left(\mathbf{U}^h\right) = \begin{bmatrix} \frac{\partial \mathbf{u}^h}{\partial \mathrm{t}} + \nabla \cdot \boldsymbol{\mathcal{N}}^{\mathrm{V}}\left(\mathbf{u}^h, \mathbf{B}^h\right) + \nabla P^h - \nu \nabla^2 \mathbf{u}^h - \mathbf{f}^{\mathrm{V}} \\ \nabla \cdot \mathbf{u}^h \\ \frac{\partial \mathbf{B}^h}{\partial \mathrm{t}} + \nabla \cdot \boldsymbol{\mathcal{N}}^{\mathrm{I}}\left(\mathbf{u}^h, \mathbf{B}^h\right) + \nabla r^h - \lambda \nabla^2 \mathbf{B}^h - \mathbf{f}^{\mathrm{I}} \\ \nabla \cdot \mathbf{B}^h \end{bmatrix}.$$

$$\boldsymbol{\mathcal{N}}^{\mathrm{V}}(\mathbf{u}, \mathbf{B}) = \mathbf{u} \otimes \mathbf{u} - \frac{1}{\mu_0 \rho} \mathbf{B} \otimes \mathbf{B}$$

$$\boldsymbol{\mathcal{N}}^{\mathrm{I}}(\mathbf{u}, \mathbf{B}) = -\mathbf{u} \otimes \mathbf{B} + \mathbf{B} \otimes \mathbf{u}$$

Sandia National Laboratories

VMS induced cross term fluxes (sub-grid to resolved scales)

$$\mathcal{N}_C^{\mathrm{V}} = \left(\mathbf{u}^h \otimes \mathbf{u}' + \mathbf{u}' \otimes \mathbf{u}^h\right) - \frac{1}{\mu_0 \rho}\left(\mathbf{B}^h \otimes \mathbf{B}' + \mathbf{B}' \otimes \mathbf{B}^h\right)$$

$$\mathcal{N}_C^{\mathrm{I}} = -\left(\mathbf{u}^h \otimes \mathbf{B}' + \mathbf{B}' \otimes \mathbf{u}^h\right) + \left(\mathbf{B}^h \otimes \mathbf{u}' + \mathbf{u}' \otimes \mathbf{B}^h\right)$$

VMS induced higher-order sub-grid term fluxes

$$\mathcal{N}_R^{\mathrm{V}} = \left(\mathbf{u}' \otimes \mathbf{u}'\right) - \frac{1}{\mu_0 \rho}\left(\mathbf{B}' \otimes \mathbf{B}'\right)$$

$$\mathcal{N}_R^{\mathrm{I}} = -\left(\mathbf{u}' \otimes \mathbf{B}'\right) + \left(\mathbf{B}' \otimes \mathbf{u}'\right)$$

- Includes subgrid effects ($\mathbf{U}'$)
- Allows for the possibility of local inverse energy cascade
- Cross stresses ($\mathbf{U}^h \otimes \mathbf{U}'$) well-represented (Wang and Oberai 2010)
- Reynolds stresses ($\mathbf{U}' \otimes \mathbf{U}'$) not adequately modeled (Wang and Oberai 2010)

  $\Rightarrow$ Eddy viscosity model?
- Mix the VMS models with an eddy viscosity model

$$\mathcal{A}\left(\mathbf{W}^h, \mathbf{U}^h + \mathbf{U}'\right) + \left(\nabla^{\mathrm{s}}\mathbf{w}^h, 2\nu_T \nabla^{\mathrm{s}}\mathbf{u}^h\right) + \left(\nabla^{\mathrm{a}}\mathbf{c}^h, 2\lambda_T \nabla^{\mathrm{a}}\mathbf{B}^h\right) = \left(\mathbf{W}^h, \mathbf{F}^h\right)$$

Eddy diffusivities

$$\nu_T = \lambda_T = \overline{C} h \sqrt{|\mathbf{u}'|^2 + \frac{1}{\mu_0 \rho}|\mathbf{B}'|^2}, \qquad \overline{C} = 0.0398$$

Oberai and Sondak, 2012

Sandia National Laboratories

Homogeneous, Isotropic Turbulence

VMS Spectral Method

- Momentum and induction cross correlation terms
- Periodic boundary conditions

  $\Rightarrow$ Only nonlinear terms
- Adds to stability of method

Further Explorations

- Detailed turbulence statistics
- Subgrid dynamo and VMS
- Helical flows
- Vary Pr_m

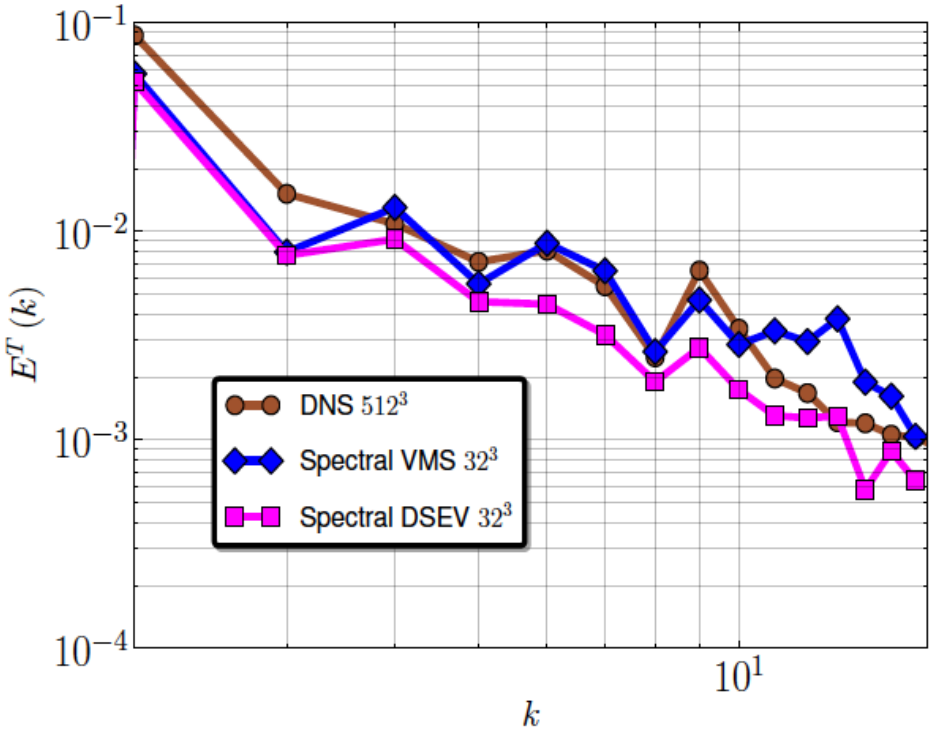

The VMS-based model performs very well. The dynamic Smagorinsky model is overly dissipative.

DNS: Pouquet et. al. (2010),
Spectral VMS: Oberai and Sondak, 2012

Sandia National Laboratories

Homogeneous, Isotropic Turbulence

VMS Spectral Method

- Momentum and induction cross correlation terms
- Periodic boundary conditions

  $\Rightarrow$ Only nonlinear terms
- Adds to stability of method

Further Explorations

- Detailed turbulence statistics
- Subgrid dynamo and VMS
- Helical flows
- Vary Pr_m

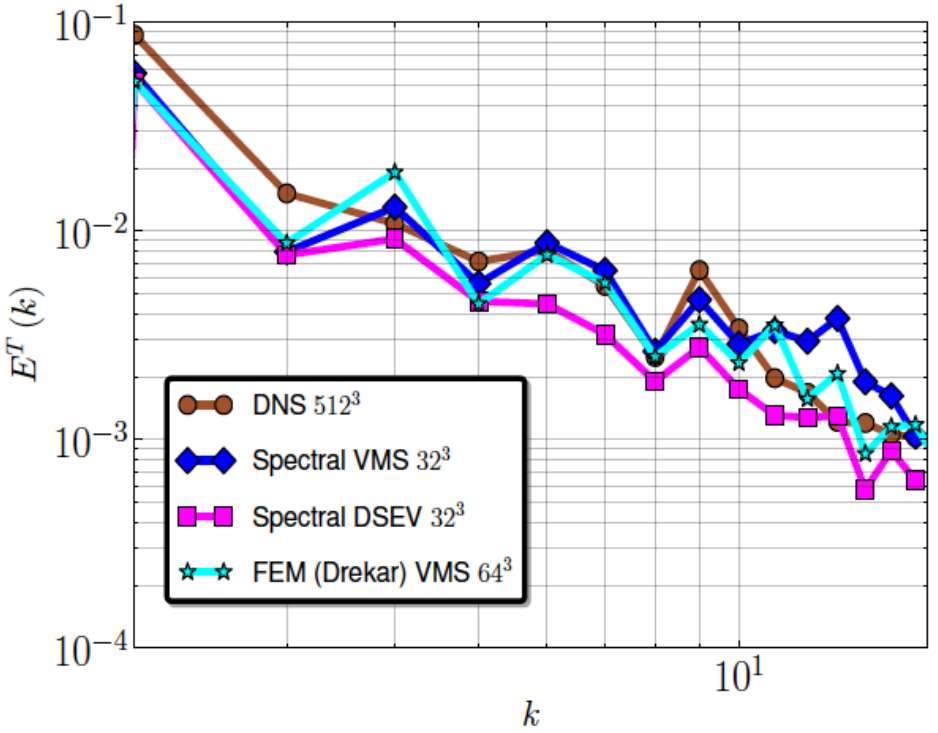

The FEM solution with linear elements using the VMS model also performs very well.

DNS: Pouquet et. al. (2010),
Spectral VMS: Oberai and Sondak, 2012

Sandia National Laboratories

Homogeneous, Isotropic Turbulence

VMS Spectral Method

- Momentum and induction cross correlation terms
- Periodic boundary conditions

  $\Rightarrow$ Only nonlinear terms
- Adds to stability of method

Further Explorations

- Detailed turbulence statistics
- Subgrid dynamo and VMS
- Helical flows
- Vary Pr_m

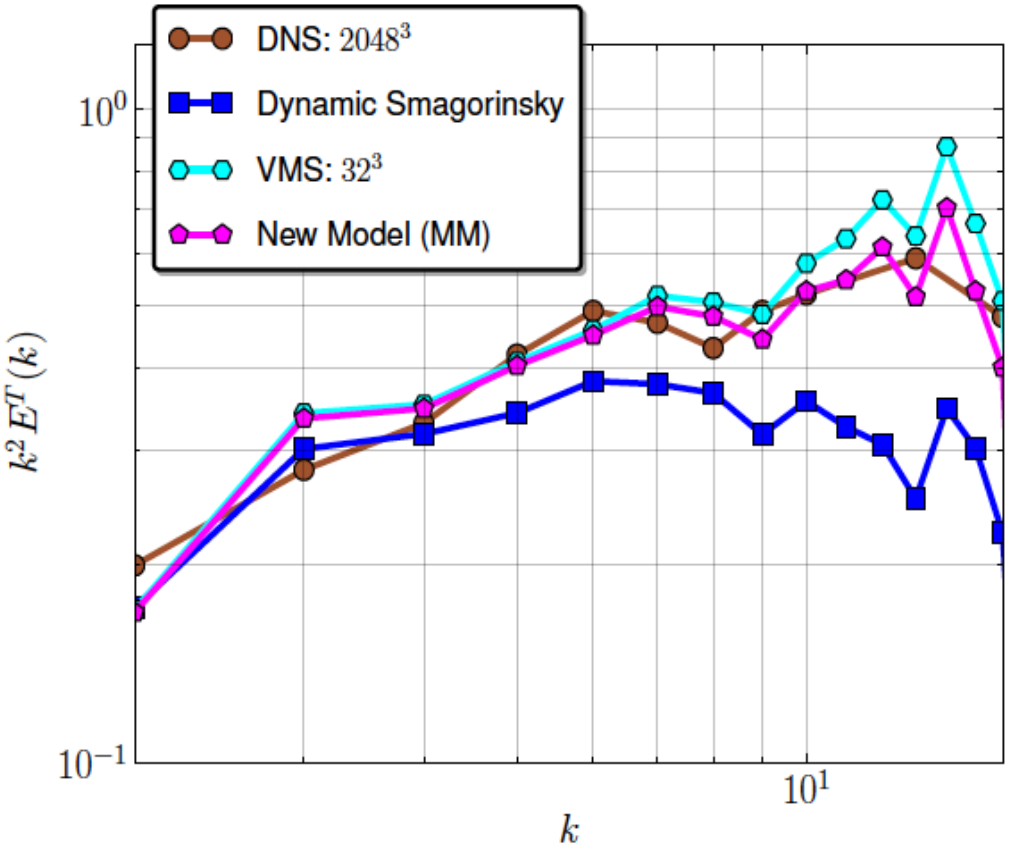

A new, VMS-based mixed model performs exceptionally well for a high Reynolds number flow.

DNS: Pouquet et. al. (2010),
Spectral VMS: Oberai and Sondak, 2012

The End

Sandia National Laboratories